Manager's Summary

ZCO-75 "Nature of Galvanizing Wettability in Advanced High Strength Steels"

Progress Report 4 : January 2018 – September 2019 (cumulative)

This report includes all wettability and adherence work carried out with a normal (GI) galvanizing bath using a DP980 and a Si-TRIP steel together with reference Ti-IF and DP600 steels. A significant amount of new work using a Zn-1.1% Al-1.1% Mg bath is also included. The experimental apparatus included the CRM Multidip simulator together with a wetting apparatus installed inside a glovebox. A standard galvanizing line condition was first used for the GI bath, namely annealing at (800°C) for 60 seconds in a 5%H_2-95%N_2 atmosphere with a dewpoint of -30°C. For the DP grades and the IF steel, good coating appearance could be obtained with this condition. Surface analysis indicated that the external selective oxidation seen with the DP steels never formed a continuous layer. This permitted the formation of a Fe_2Al_5 inhibition layer which had enough continuity to permit good wetting behavior. A 90° bend test using an automotive adhesive always showed good coating adhesion for the reference galvanizing condition. Improved wettability was obtained for each of these grades using a dew point of 0°C. A more continuous inhibition layer was seen in this case. The addition of a preoxidation step using 1%O_2 - 95%N_2 gas, with preoxidation at either 650°C or 700°C before the annealing step, further improved zinc wettability and the density of the inhibition layer without deteriorating zinc adhesion. Decarburization depths with the DP steels never exceeded around 2µm. For the TRIP steel, a quench and partition thermal cycle utilizing an annealing temperature of 870°C for 120 seconds was used. In this case, good wetting and coating adhesion could only be obtained with the high dew point without any preoxidation step. With the low dew point atmosphere wettability and coating appearance were poor. This wettability could be improved by addition of a preoxidation step at either 650°C or 750°, however, adhesion then became very poor. The decarburization depth of the high dew point treated samples, with a preoxidation step, increased to about 40 µm for the TRIP steel. The improvement wettability of the pre-oxidized samples with the 0°C dewpoint soaking helped control the surface oxide thickness layer, permitting a a suitable reduced iron layer to be produced; the use of this 0°C dew point soak together with the preoxidation step improves wettability because internal oxidation is promoted, together with development of a surface iron oxide layer that can later be reduced. Experimental evidence shows that iron oxide thickness increases with oxidation temperature and dew point. The higher iron oxide thickness delays diffusion of the reactive alloy elements (Mn,Si) to the top surface. The high dewpoint however, greatly impaired coating adhesion when used together with preoxidation. It was observed that the inhibition layer formed over external Mn-Si oxides. These oxides produced a thin but weak interface, greatly reducing the adhesive strength. This is interpreted as occurring because during iron oxide reduction Si, Mn can segregate at the reduced iron /steel interface because silicon cannot diffuse through the Fe_2O_3

(hematite) layer. Also, the dew point at the reduced iron/steel interface is much lower than on the top surface because of the small amount of oxygen that is diffusing through the reduced iron, therefore, the oxygen partial pressure at the reduced iron/steel interface is not the expected 0°C, but significantly lower. This is expected to encourage external oxidation conditions for silicon at the reduced iron/steel interface and induce silicon oxide segregation at this interface.

Work using a Zn-1.1% Al -1.1% Mg bath utilized the same steel grades. An interesting observation using the multidip simulator was the relative height of the wetted area after dipping in the simulator. These could be directly related to the quality of coatings that were observed. The surface oxides on the Zn-Al-Mg bath could be repelled if wettability of the tested steels was satisfactory, however, if poorly wetted areas were produced, the oxides were strongly attracted into these areas producing oxide defects in the coating.

The nature of the inhibition layer and its relationship to wettability with the Zn-Al-Mg coating follows the same relationship as seen with the GI coatings with thinner, more concentrated, fine grained characteristics of the inhibition layer being associated with good wettability. Zinc's spreading behavior was found to be very different for the Zn-Al-Mg bath than the GI bath. In the case of GI, the Fe_2Al_5 layer is to be stabilized with time, because of the strong Fe-Zn reactivity. This does not occur in the Zn-Al-Mg bath because of the high Al content which helps keep the Fe_2Al_5 layer stable. There is also conjecture that the Al-Mg oxides surrounding the liquid droplet can further block reactivity and zinc spreading. The steels reacted to the pretreatment conditions in the same way for these experiments as in the GI experiments, producing the same intensity of internal and external oxidation before dipping, however, in these experiments, less decarburization was seen with the DP980 steels than the other grades. There are still some questions regarding the nature of internal vs external oxidation and how this relates to the formation of the inhibition layer in the DP980 steel, as explained in the report. For the TRIP steel using the quench and partition pretreatment process, good wettability behavior could be obtained, together with acceptable coating adhesion at the 0°C dew point. However, use of the oxidation process greatly deteriorated coating adhesion for this steel grade, although a very good coating adherence could be achieved. The same mechanism of formation of a Si-Mn oxide layer at the coating interface, below the inhibition layer seen in the GI coatings accounts for this behavior.

CENTRE FOR RESEARCH IN METALLURGY

Avenue du Bois St Jean, 21
Domaine Universitaire du Sart-Tilman (P59)
BE - 4000 LIEGE
Phone : +32 4 254.62.11
Fax : +32 4 254.62.62

CRMG-108-F

09/09/2019

CONFIDENTIAL

ZCO-75: "Nature of Galvanizing Wettability on Advanced High Strength Steels"

Report n°4

Private research

Period: 01/2018 – 12/2019

Research Leader : L. Bordignon
Project Associates :

N°CRM: RPI2017059

Hot dip galvanising of 3G steels

1. Objectives

The objective of this program is to explore the limits of wettability of advanced high strength steels, primarily focusing on steels that have been prepared using an oxidation-reduction treatment prior to hot dipping, with significant attention paid to the nature of the substrate surface at the point of hot dipping. The study will be limited to selected dual-phase steels, together with a control composition of a simple IF steel.

2. Introduction

2.1. Steel composition

A DP980 and a TRIP-Si have been selected for the whole program (Table 1). As requested, an IF Ti will be used as a reference. However, the real question is: how to transpose the wetting angle, measured by the sessile drop method, to the zinc reactivity in industrial configuration? Indeed, wetting improvement will be observed with an adapted atmosphere composition, but will it be sufficient to guarantee a good galvanisability on industrial lines? Therefore, a DP600 should also be added as a reference because this alloyed steel grade, should be correctly galvanized in all lines without adaptation of the atmosphere composition. Consequently, for being acceptable for industrial application, all the modified atmosphere conditions should allow obtaining zinc wetting angles at least lower than the one measured for the DP600, while being as close as possible to the IF Ti measurements after a standard annealing (800°C/ 60s / 5%H_2 / DP-30°C).

Table 1: Steel composition (wt%)

	C	Si	Mn	Cr	Al	P	Mo	Nb	Ti
DP600		0.230	1.700	0.450					
DP980	0.092	0.490	2.259	0.336	0.050	0.021	0.205	0.038	0.029
TRIP Si	0.210	1.628	1.718	0.032	0.030	0.013	< 0.005	0.007	0.008

2.2. Proposed program

The proposed program is schematically summarized in Figure 1 . It is intended to:

- Study the influence of an oxidation/reduction process or an internal oxidation in comparison with a classical annealing condition.
- Determine their influence on zinc wetting and coating adhesion.

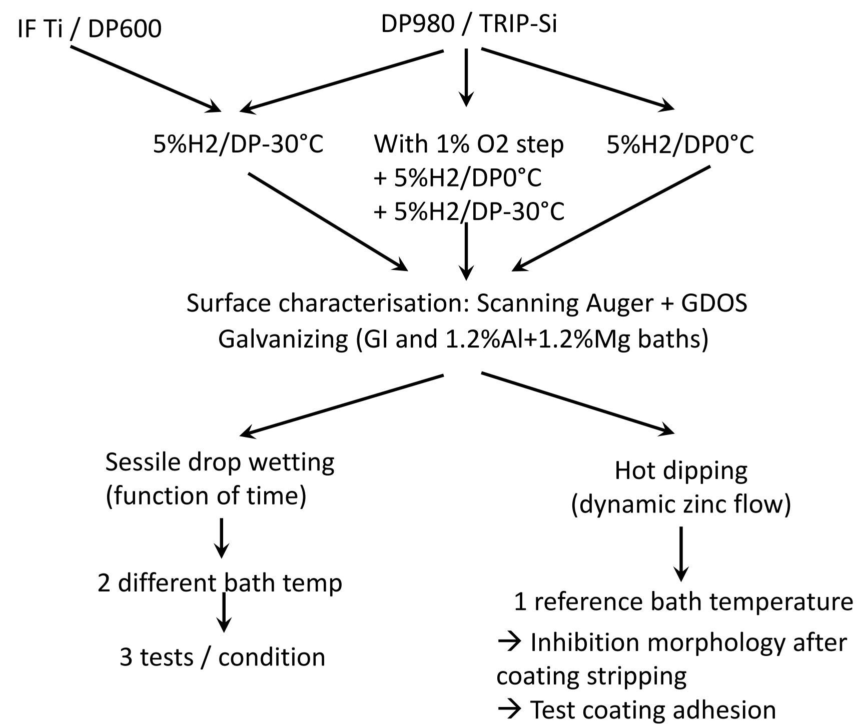

Figure 1: Schematic program proposed

3. Experimental procedure

The multidip simulator (Figure 2) was used for studying the influence of various annealing atmospheres on the coatability. This simulator is equipped with 2 infrared furnaces. The top one is used for strip preparation in oxidizing atmospheres, while the bottom one can be used to pre-heat the samples or to finish the strip conditioning before hot dipping in more classical atmospheres.

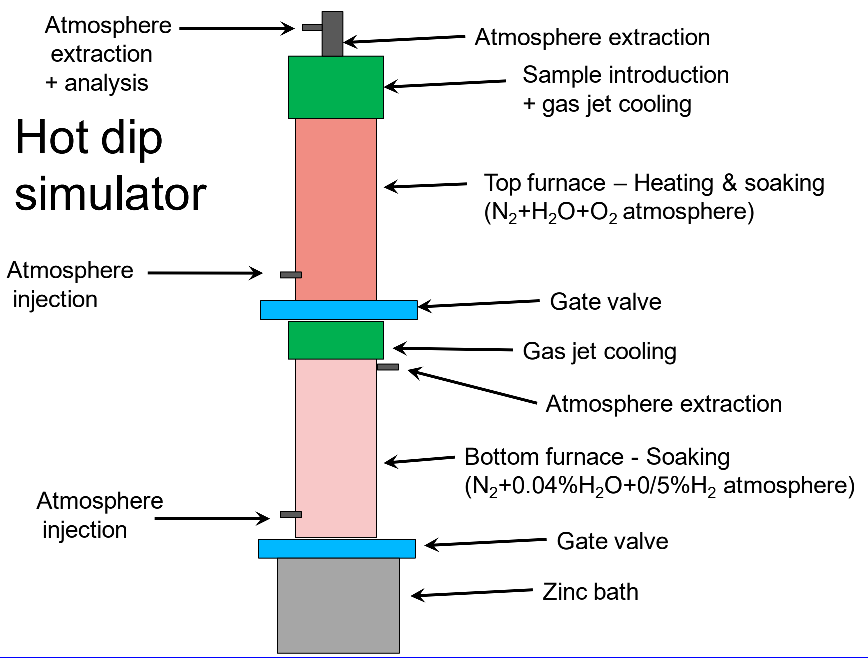

Figure 2: Schematic view of the Multidip simulator.

A classical annealing cycle (800°C/60s) will be applied on the DP980 steel grade as well as on the reference steel grades. A Q&P annealing cycle was chosen for the TRIP-Si steel to study the influence of higher annealing temperatures (870°C/120s).

The wetting measurements are performed by a dedicated equipment installed in a glove box (Figure 3). The thermal cycle is controlled by an infrared furnace with the desired atmosphere. The sample is deposited on a hot plate to keep it at the correct temperature (460°C in this case) before depositing the GI droplet at 460°C. 100 pictures are recorded during the droplet spreading and the wetting angle is measured as reported in Figure 4.

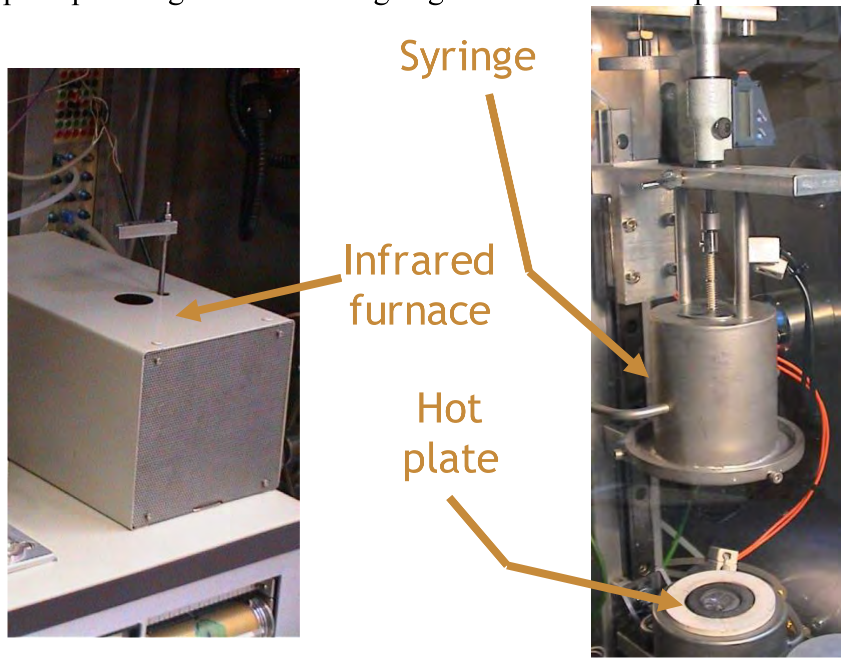

Figure 3: Pictures of the sessile drop equipment

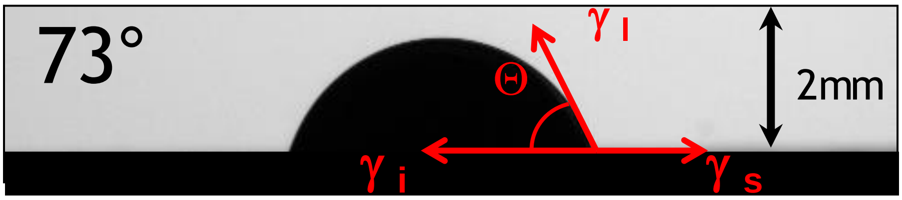

Figure 4: Example of picture of zinc droplet

4. Coatability with the GI bath

4.1. <u>Coatability of the DP980 steel</u>

The DP980 steel has been galvanized with the 2 reference steel grades (IF Ti / DP600) under classical annealing conditions (800°C/60s/5%H_2/DP-30°C).

Figure 5 gives an example of the thermal cycle applied on the DP980 steel with an oxidation step in the top furnace of 3 seconds at 650°C with 1%O_2 and a soaking made with standard dew point (-30°C) or at a high dew point (0°C) in the bottom furnace.

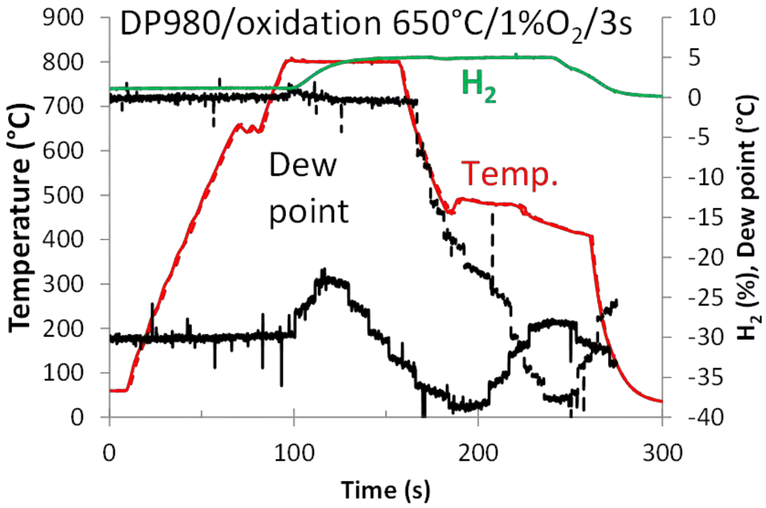

Figure 5: Thermal cycles and associated gas analyses in the bottom furnace during the annealing at two different dew points (-30°C / 0°C), with a 3 seconds oxidation step in the top furnace.

Good coating aspect was always observed for the 2 dual phase steels.
This means that Mn/Cr/Si external oxidation (Figure 6) do not completely cover the steel surface, which allows a sufficient reactivity for zinc wetting.
The GDOS in depth profile, made after annealing, shows that if water vapour injection already allows reducing external selective oxidation for the DP980 steel, pre-oxidation brings much more additional improvement of the surface preparation (Figure 7).
Figure 8 indicates that the injection of water vapour clearly promote zinc wetting for the DP600. The wetting of the DP980 is very close to the wetting behaviour of the DP600 steel after standard annealing, which explains the absence of bare spots on the galvanized panels. The injection of water vapour only slightly improves the wettability of the DP980 during the 3 first seconds.
It has to be remembered that the wetting behaviour has to be located between the one of a DP600 and an IF Ti steel to warrantee a coating without bare spots.
This slight wetting improvement with water vapour injection is correlated for the DP980 with the insufficient decrease of the Mn-Si external selective oxidation observed on the GDOS profiles (Figure 7). Only the Chromium external selective oxidation is strongly diminished.
An oxidation step during heating gives additional wetting properties (Figure 9), but the wetting angle is never as low than the one observed for the IF Ti during the 3 first seconds. This is probably explained by the presence of a more important external selective oxidation, even after an oxidation step.
This wettability has also to be associated with the formation of the inhibition layer, which has been characterized by GDOS (Figure 10) and SEM observations (Figure 11) after electrochemical stripping of the zinc coating. A fine and covering inhibition layer is observed on the IF Ti steel grade. The inhibition becomes coarser for the alloyed steel grades after annealing in reference conditions (800°C/60s/5%H_2/DP-30°C). Some areas are not covered with Fe_2Al_5 due to the presence of a too important selective oxidation before hot dipping. The introduction of an oxidation step during heating clearly improves the homogeneity of the inhibition layer (Figure 10 and Figure 12), which confirms that less external selective oxidation covers the steel surface before hot dipping (Figure 7).

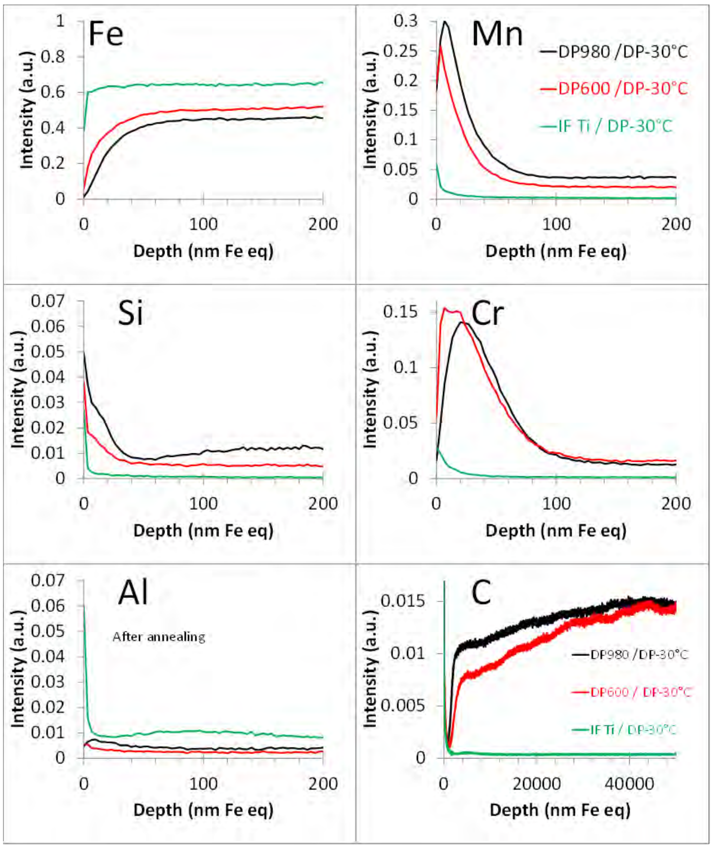

Figure 6: GDOS indicates Mn/Cr/Si external selective oxidation after annealing in classical conditions (5%H_2/DP-30°C).

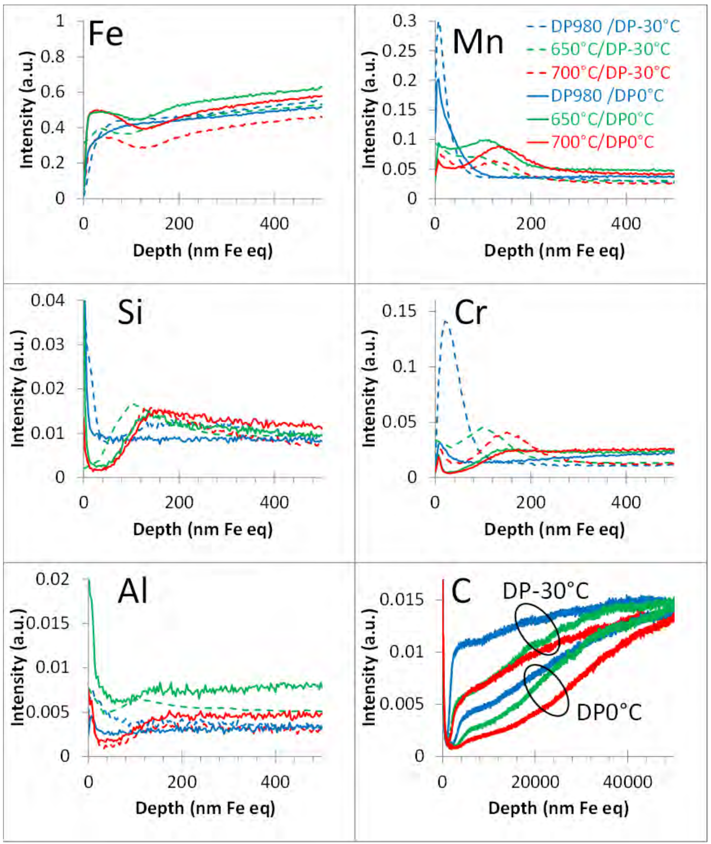

Figure 7: GDOS shows that water vapour injection already allows reducing external selective oxidation, but pre-oxidation brings additional improvement.

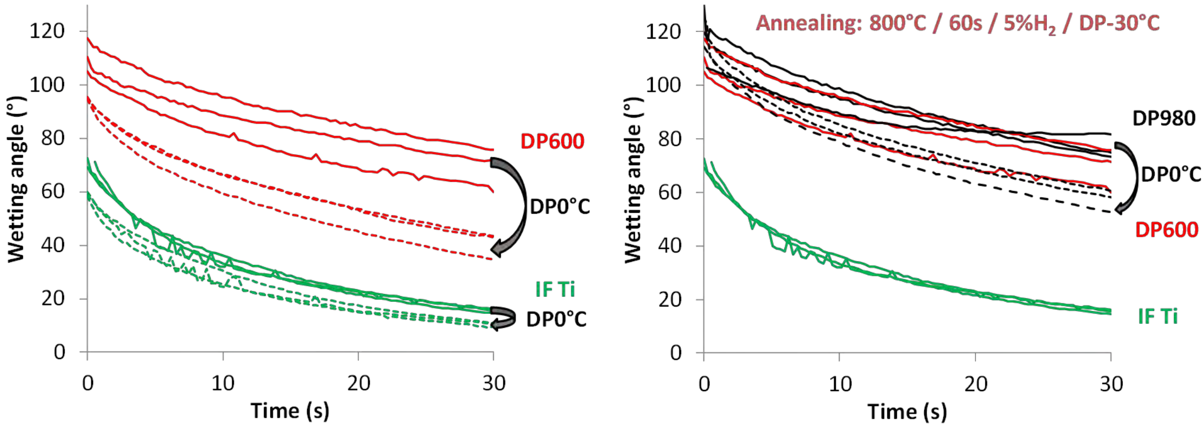

Figure 8: The injection of water vapour clearly promote zinc wetting for the DP600 but the improvement is weak during the first 3 seconds for the DP980

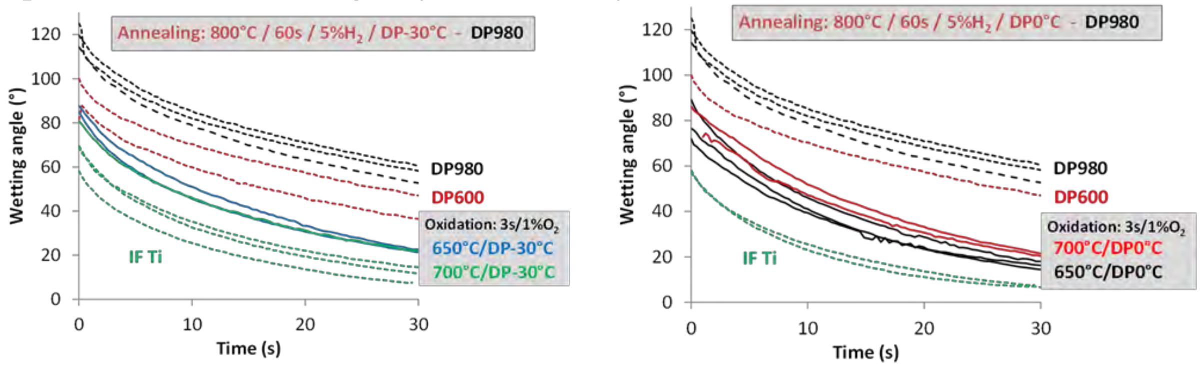

Figure 9: An oxidation step allows to significantly improving zinc wetting for the DP980.

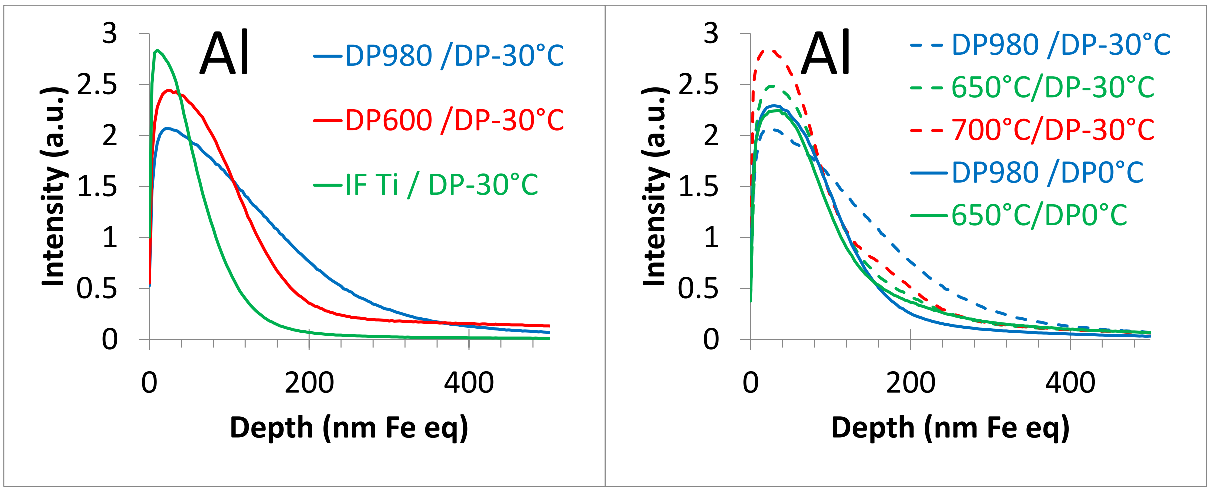

Figure 10: GDOS profiles after electrochemical dissolution of the zinc layer: Sharp Al profile for IF-Ti steel or for pre-oxidized DP980 grades, indicating a fine and continuous inhibition layer.

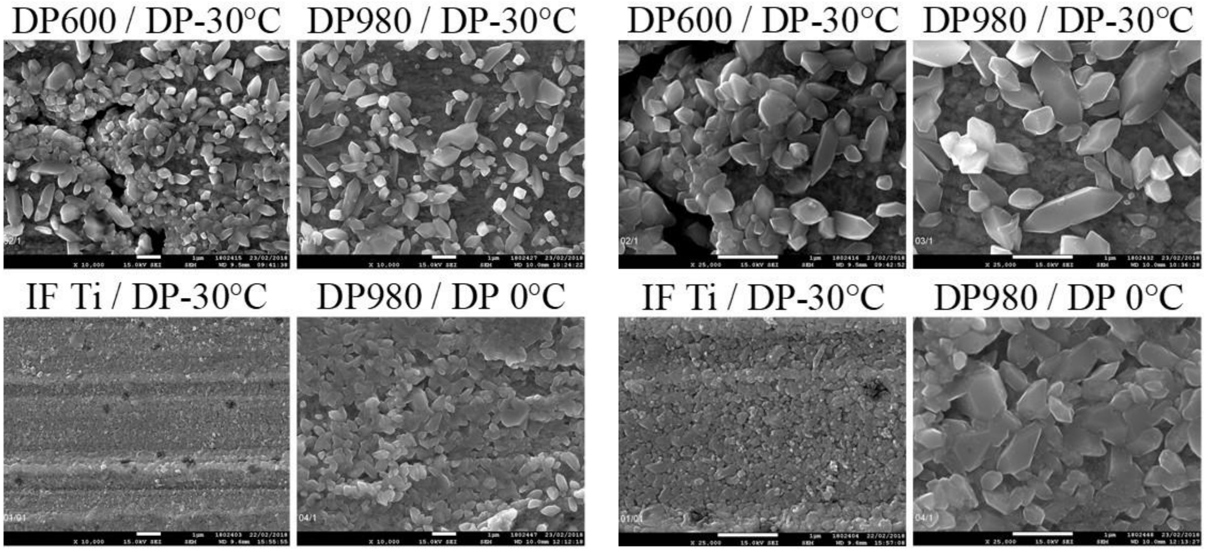

Figure 11: SEM images of the inhibition layer after electrochemical dissolution of the zinc layer: a more dense inhibition layer is observed on the IF Ti steel grade, but w ater injection allows increasing the homogeneity of the Fe_2Al_5 for the DP980.

The SEM image of the inhibition layer after an oxidation at 700°C/DP0°C is strange and not in line with the wetting measurements (Figure 9). It seems that the Fe_2Al_5 layer has been delaminated by the electrochemical dissolution. The more important residual reduced iron layer obtained for this oxidation condition and located between the inhibition layer and the base steel is perhaps not stable for the pickling conditions.

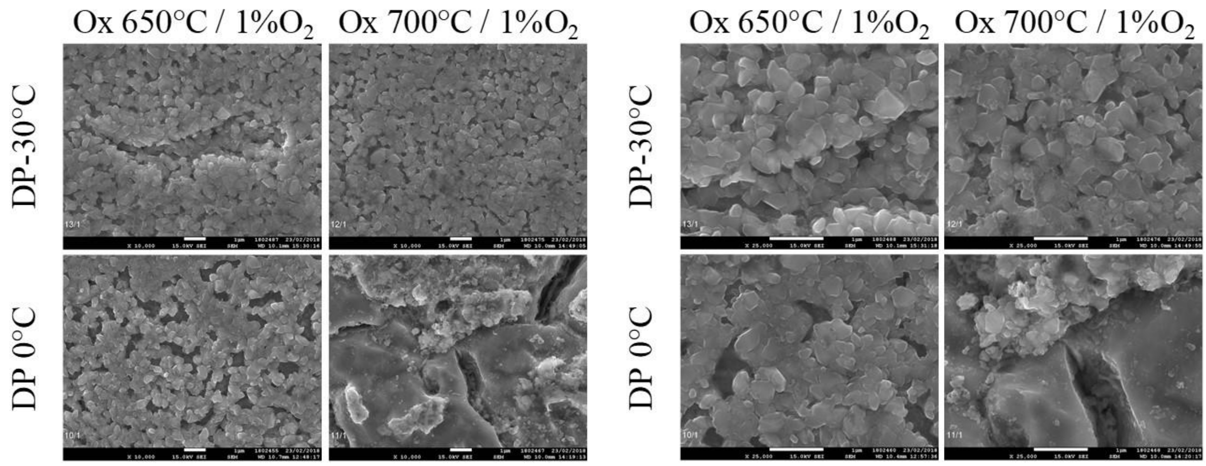

Figure 12: Better inhibition layer repartition after an oxidation / reduction process (the dissolution after an oxidation at 700°C with a dew point of 0°C has to be done again).

Finally, the carbon profiles in Figure 7 indicate that the oxidation step induces an additional decarburizing to the important influence of the dew point during soaking. The thickness of this oxidized layer is relatively stable (Figure 13 - Table 2) when the oxidation is made between 650°C and 700°C with 1%O_2 and a dew point of -30°C or 0°C. It can be estimated to 1.3 g/m², which is close to our maximum target.

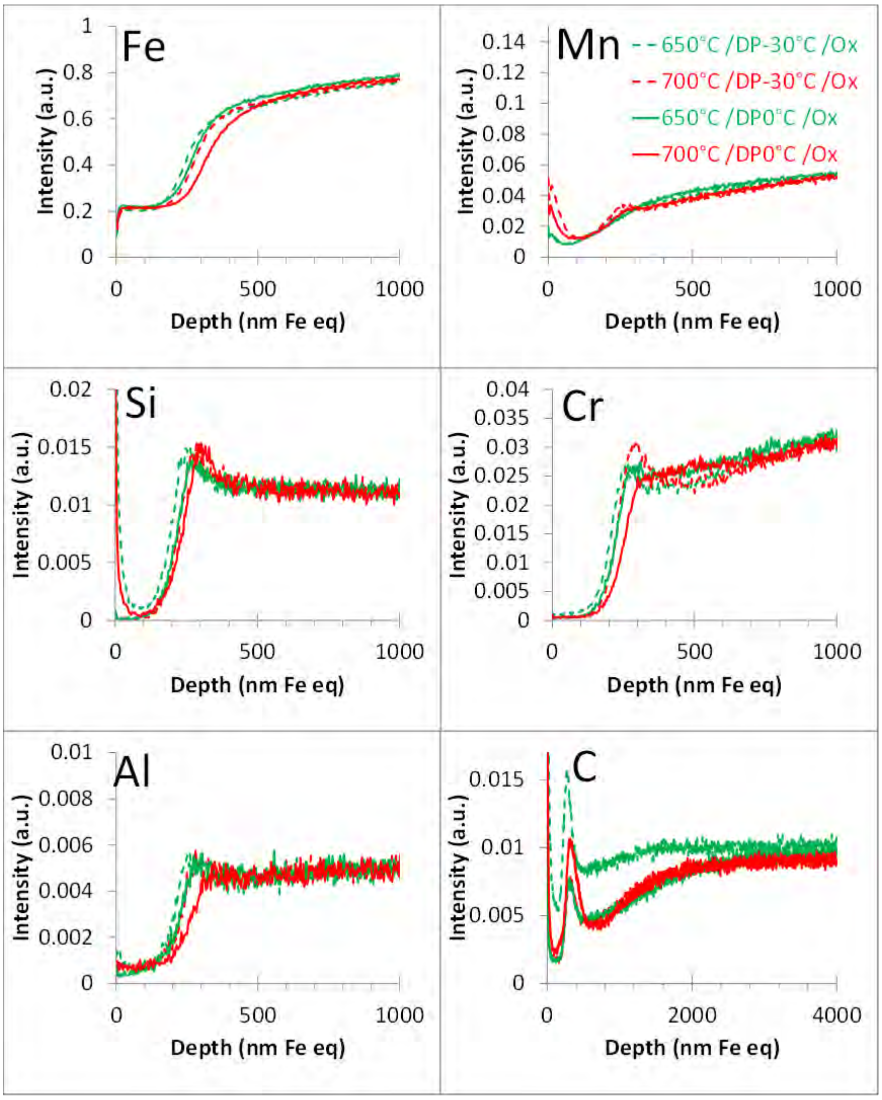

Figure 13: GDOS, made after the oxidation step, indicates an oxide thickness of around 1.2 g/m² after oxidation with 1%O_2 during 3s for the DP980 steel grade.

Table 2: Oxide thickness (g/m²)

	650°C		700°C	
	DP-30°C	DP0°C	DP-30°C	DP0°C
DP980	**1.16**	**1.26**	**1.30**	**1.45**

Some Mn/Cr/Si oxides however segregate behind the inhibition layer (Figure 14), especially after an oxidation at higher temperature, which could also weaken the coating adhesion.

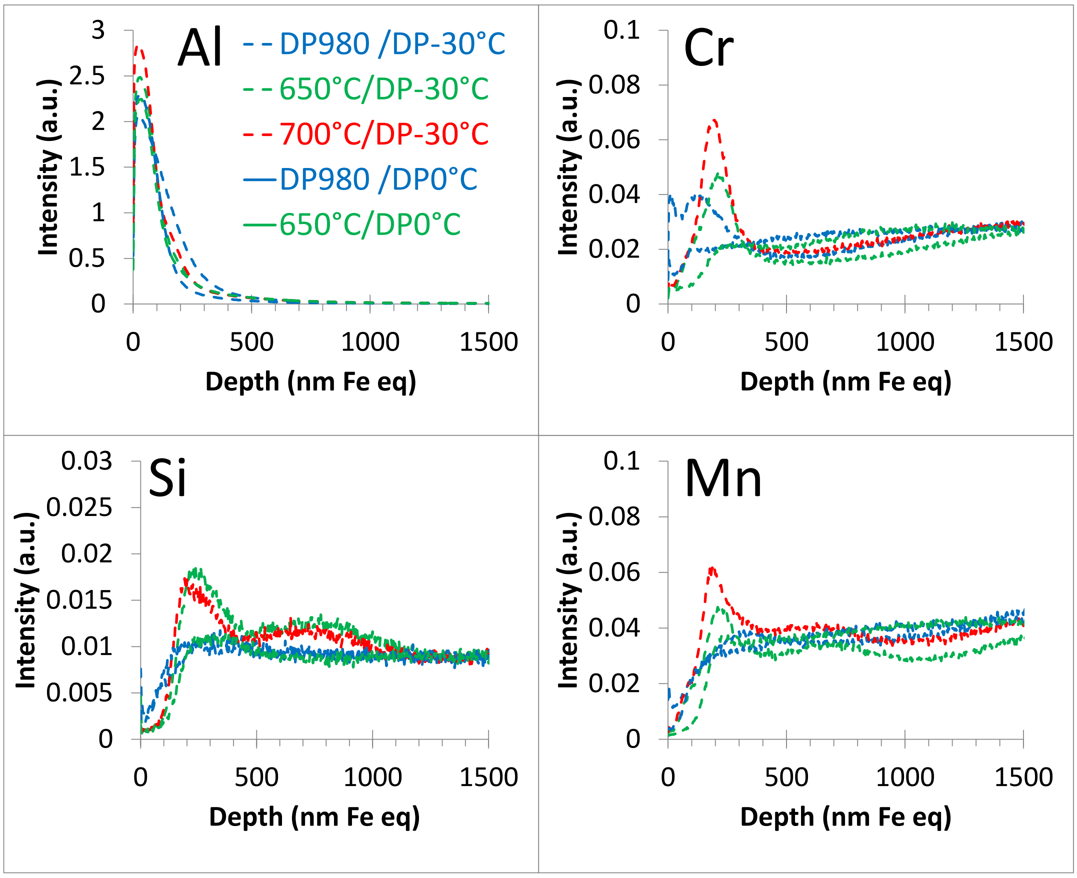

Figure 14: GDOS profiles after electrochemical dissolution of the zinc layer made on the galvanized DP980 with/without an oxidation step and with/without water vapour injection.

Adhesion tests have been made to determine if theses segregations can alter coating adhesion. The 90° bending test was made after the application a glue (betamate) on the coating to increase delamination stresses. The pictures in Figure 15 show the glue side after it's decohesion from the coating. In the case of a poor adhesion, the coating sticks on the glue. According to these figures, no zinc coating de-cohesion is observed neither on the reference steel grades (IF Ti and DP600) nor on the DP980 steel grade whatever the annealing conditions (with/without oxidation and with/without water vapour injection).

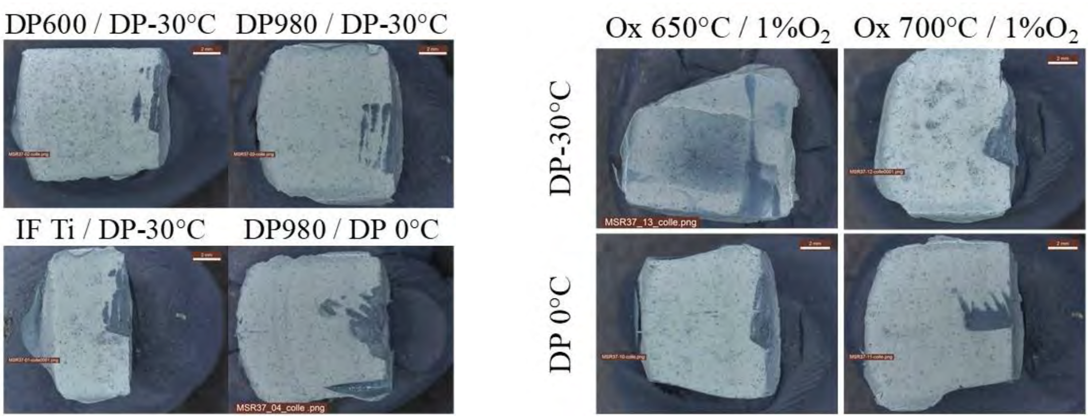

Figure 15: No zinc sticks on the glue side after classical annealing conditions with or without water vapour injection or with an oxidation step, which indicates a good coating adhesion.

4.2 Coatability of the TRIP-Si steel

A full austenitic Q&P annealing cycle has been applied on the TRIP-Si steel as reported in Figure 16.

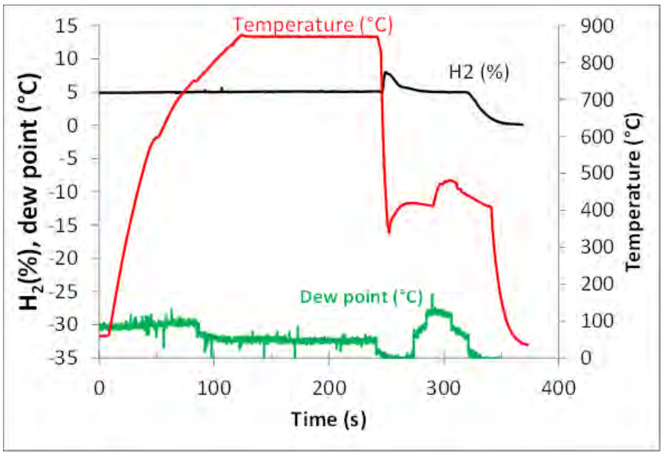

Figure 16: Thermal cycles and associated gas analyses in the bottom furnace during the annealing in the reference conditions.

Figure 17 indicates that after such reference annealing treatment, important Mn-Si oxides covers the surface because quite no iron is detected on the first 50nm for the TRIP-Si.

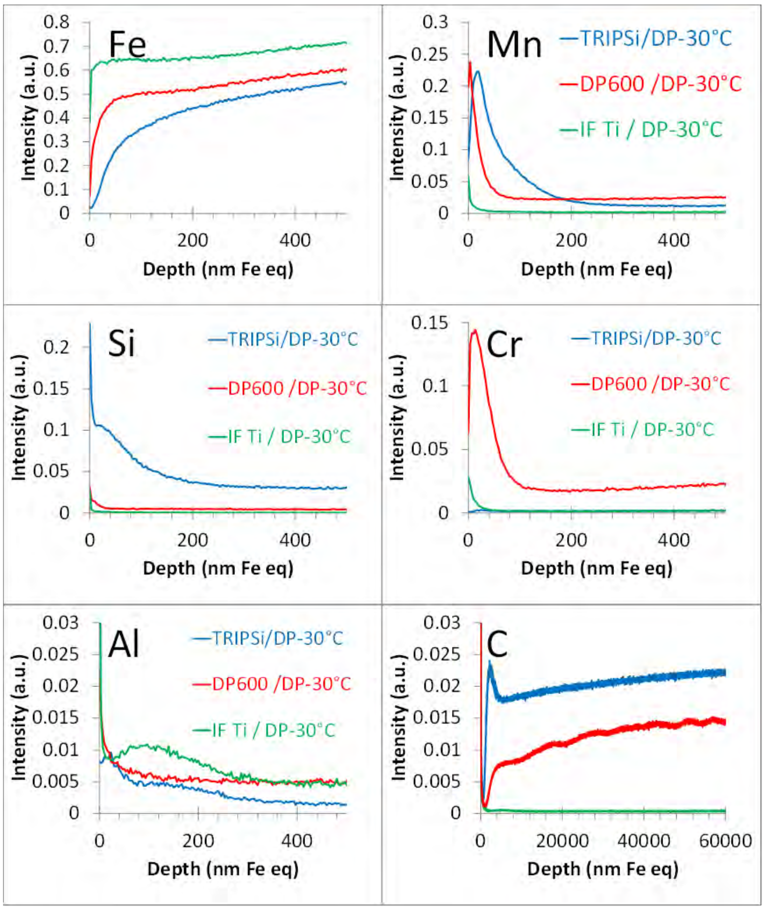

Figure 17: GDOS indicates Mn/Cr/Si external selective oxidation after annealing in reference conditions (5%H_2/DP-30°C).

Figure 18 shows that a correct iron signal, associated very low Mn-Si external oxidation is obtained with an oxidation / reduction process followed by a soaking at high oxidation potential (DP0°C / 5%H_2).
A soaking at low dew point, coupled with an oxidation step of 3seconds, is less efficient for decreasing the amount of external Mn-Si oxides.
Without this total oxidation step, a soaking at high dew point can already reduce silicon oxidation.
Finally, as observed for the DP980 grade, an important decarburizing is noticed after soaking at high dew point. An additional effect of the oxide thickness can also be seen.

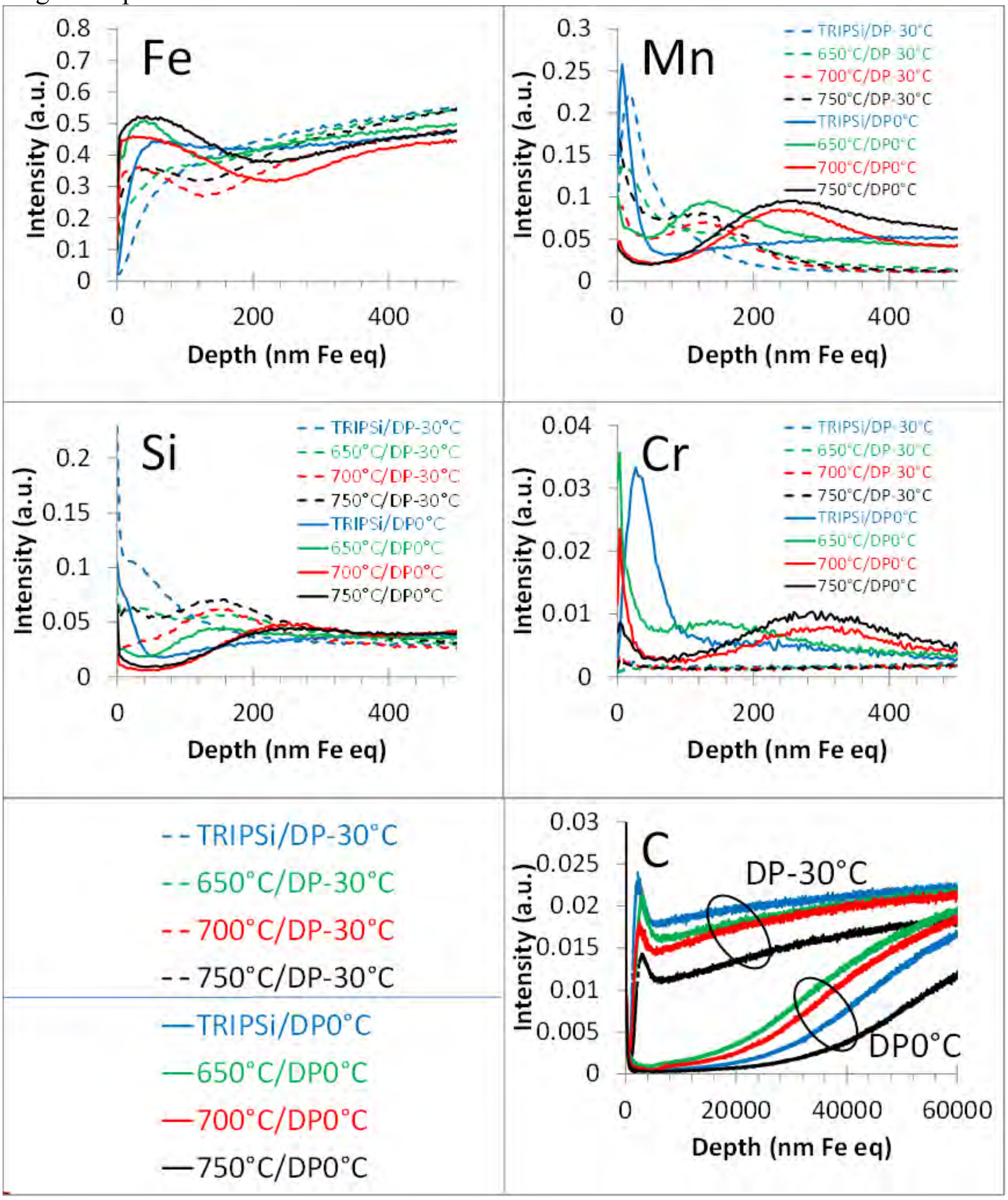

Figure 18: GDOS shows that water vapour injection already allows reducing external selective oxidation, but pre-oxidation brings additional improvement.

The quite complete surface coverage with Mn-Si oxides on the TRIP-Si grade, after standard annealing, induces a poor reactivity (Figure 19) and leads to poor GI wetting as reported in Figure 20. Indeed, the Al peak in Figure 19 corresponds to the presence of the Fe_2Al_5 inhibition layer. An intense and thin profile indicates a perfect inhibition layer with a good surface coverage like it is the case for the IF Ti steel. When coarser grains are formed, the Al profile becomes larger as it is the case of the DP600 steel. In the case of the TRIP-Si, the GDOS Al profile point out the presence of a very poor inhibition layer.

The decrease of this external selective oxidation, obtained with an annealing at high dew point, significantly improves zinc wetting (Figure 21). The wetting is now close to the one obtained for the DP600 annealed in standard conditions, which means that no bare spots should be observed after hot dipping.

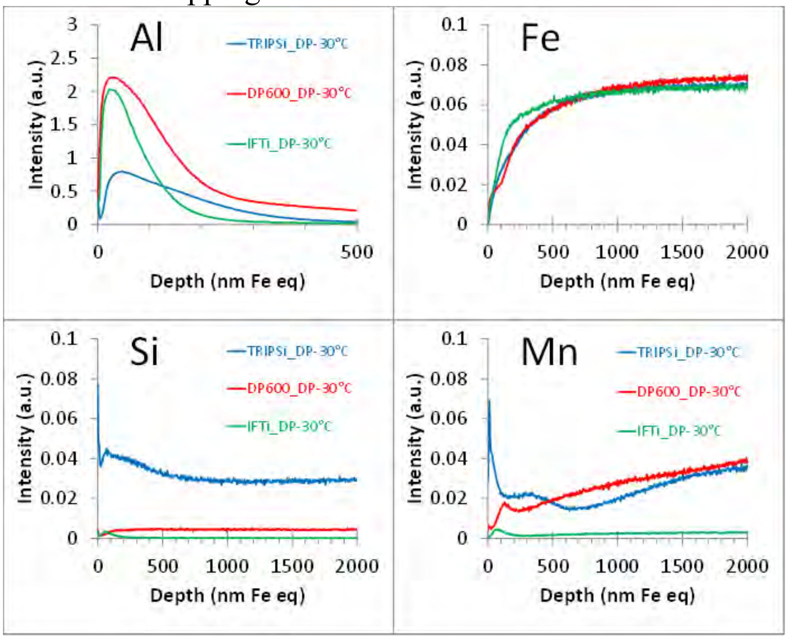

Figure 19: GDOS profiles after electrochemical dissolution of the zinc layer covering the different steel grades (annealing 870°C/120s/5%H$_2$/DP-30°C) shows an insufficient inhibition layer on the TRIP-Si steel (too weak Al signal).

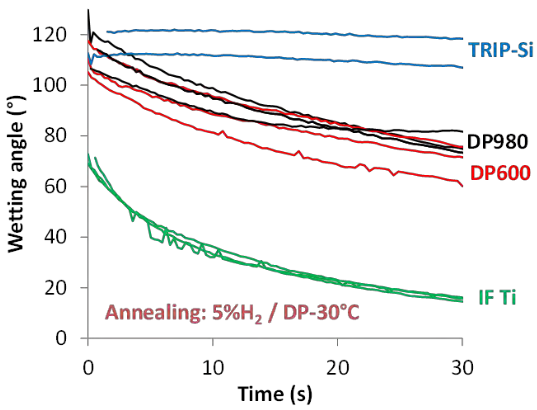

Figure 20: The wetting behaviour has to be located between the one of a DP600 and an IF Ti steel to warrantee a coating without bare spots. The TRIP-Si steel has a poor wetting behaviour after annealing in standard conditions.

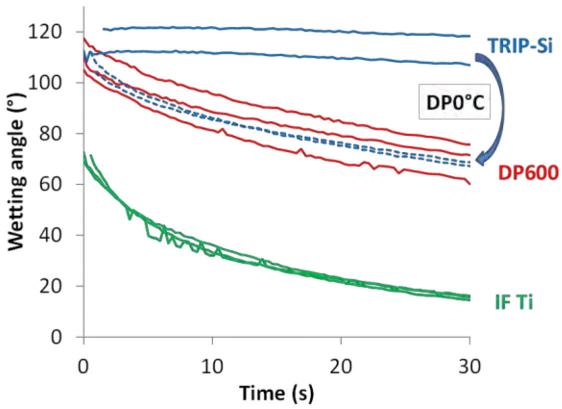

Figure 21: The injection of water vapour clearly promote zinc wetting on a TRIP-Si steel annealed at 870°C/120s/5%H₂.

The wetting improvement obtained with an oxidation step (Figure 22) is insufficient if the annealing is made with a classical dew point (DP-30°C) and at low temperature (650°C). After an oxidation at 700°C, the wetting becomes acceptable, which means that a minimum oxide thickness is needed to stabilize a correct reduced iron layer.

However, if this oxidation step is associated with an annealing at high dew point, an additional wetting progress is reached. The water injection participates to iron oxide formation but also promote internal oxidation.

Figure 23 and Table 3 indeed indicate that the iron oxide thickness increases with the oxidation temperature and the dew point. A higher iron oxide thickness should delay the possible segregation of alloying elements to the top surface. The difference of iron oxide thickness can however not explain the wetting difference after a soaking made at low or high dew point. Therefore, a high dew point during soaking seems to be very efficient for preventing further diffusion of alloying elements to the top surface.

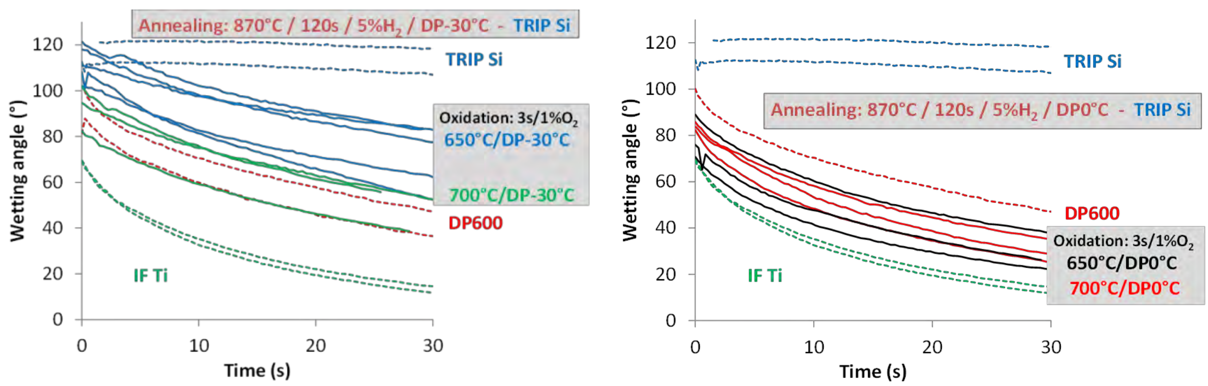

Figure 22: The injection of water vapour combined with an annealing at high dew point allows obtaining the best zinc wetting on the TRIP-Si steel grade. An oxidation at low temperature before an annealing in standard conditions is insufficient for the good wettability of this steel grade.

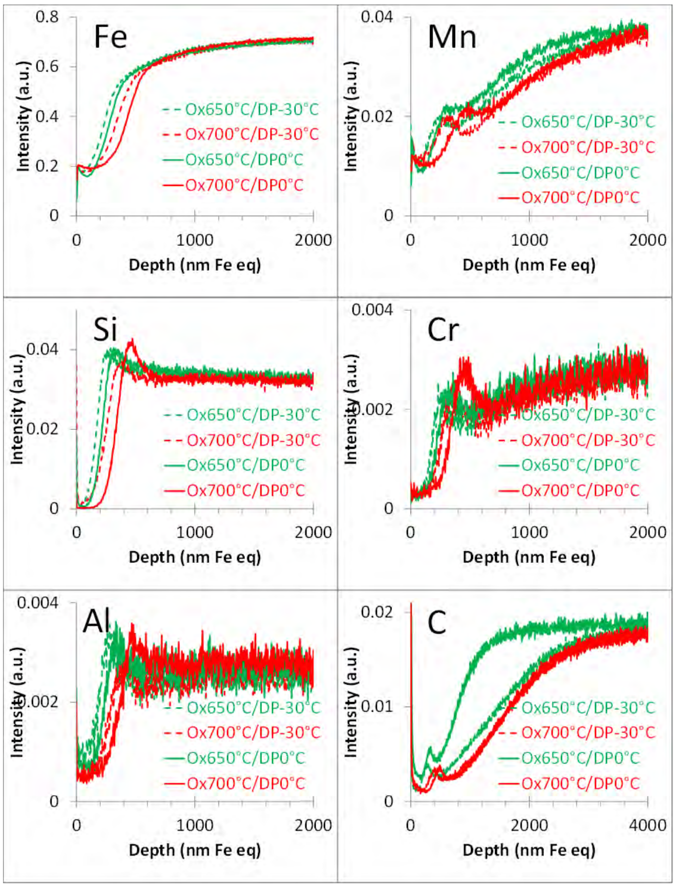

Figure 23: GDOS in depth profiles, made after the oxidation step, indicate that the iron oxide thickness increases with oxidation temperature and dew point for the TRIP-Si steel.

Table 3: Oxide thickness (g/m²)

	650°C		700°C	
	DP-30°C	DP0°C	DP-30°C	DP0°C
DP980	**1.16**	**1.26**	**1.30**	**1.45**
TRIP-Si	**1.18**	**1.32**	**1.59**	**1.91**

This wetting improvement is associated with an intense and narrow Al profile (Figure 24), corresponding to the formation of a good inhibition layer. We can however notice that in the case of the oxidation at 700°C / DP0°C, quite no Al peak is formed, which is probably an artefact of preparation. Indeed, during the electrochemical dissolution of the metallic zinc, the selective oxidation is also removed. In an oxidation / reduction process, the inhibition layer can be formed on the reduced iron oxide, while keeping Si/Mn oxide at the interface with the steel substrate. If the pickling solution can access to this oxide, their dissolution will also induce a de-cohesion of the covering inhibition layer from the base steel surface leading to the absence of Al signal in the GDOS profile.

We can also notice that the simple water vapour injection induces the formation of a more intense Al signal, but with a large peak, which means that big Fe_2Al_5 crystals should be observed.

In this more classical process without ox/red process, the inhibition layer only growth between the selective oxidation. After electrochemical preparation, these selective oxides will be dissolved and the SEM observation will only show some voids between the Fe_2Al_5 crystals.

Figure 25 indeed exhibit big Fe_2Al_5 crystal at DP0°C, but much more numerous than at DP-30°C on the TRIP-Si steel, where quite no inhibition layer is observed. The amount and shape

of these crystals at DP0°C are approximately the same that on the DP600 steel annealed at DP-30°C, which explains the same wetting behaviour noticed in Figure 21.
Figure 26 shows very complex Fe_2Al_5 structures if an oxidation step is introduced during annealing. This complex structure is probably related to the preparation artefact previously described.
To test coating adhesion, the 90° bending test was made after the application of glue (betamate) on the coating for increasing delamination stresses. The pictures in Figure 27 show the glue side after the bending test. In the case of a poor adhesion, the coating sticks on the glue. Such bad coating adhesions are observed if an oxidation step is introduced in the annealing cycle (Figure 27). Surprisingly, a good coating adhesion is noticed with an oxidation at 700°C followed by an annealing at DP0°C. It is perhaps due to a bad application of the glue?
Auger mapping, made at the steel / coating interface (Figure 28), shows that the inhibition layer is formed over a Mn-Si oxide. These selective oxides make a thin but weak interface, which completely destroy coating adhesion. SEM-EDX analyses made on the Glue side and the corresponding steel side (Figure 29) clearly shows that the coating delamination observed after the bending test is located around the Si/Mn oxide.
This situation can be obtained if an oxidation step is applied during annealing. During the iron oxide reduction, Si/Mn can segregate at the reduced iron /steel interface because silicon cannot diffuse through the Fe_2O_3 layer. Another interpretation needs to consider that the dew point at the reduced iron /steel interface is significantly lower than on the top surface due to the needed oxygen diffusion through the reduced iron. Therefore, the oxygen partial pressure is not the one corresponding to a dew point of 0°C but significantly lower. This could induce external oxidation conditions for silicon at the reduced iron/steel interface and induce Silicon oxide segregation along this interface.
The same problem was also encountered during the previous ZCO54 study with a 1.5%Mn/1.5%Si steel during annealing in oxidation conditions (N_2+500ppmO_2). Figure 30 indeed indicates that Si/Mn oxides segregation at the Fe_2Al_5/steel interface were at the origin of the bad coating adhesion. The problem was however solved when water vapour was added during this oxidizing annealing treatment (DP0°C instead of DP-60°C). Indeed, this additional water vapour injection allows transferring Silicon oxidation to the internal mode (Figure 31).

According to Figure 27, no zinc coating de-cohesion is observed neither on the reference steel grades (IF Ti and DP600) nor on the TRIP-Si steel grade annealed at DP0°C. A bad adhesion can be however noticed on TRIP-Si after annealing at DP-30°C, which is consistent with the poor inhibition layer obtained for this annealing condition.

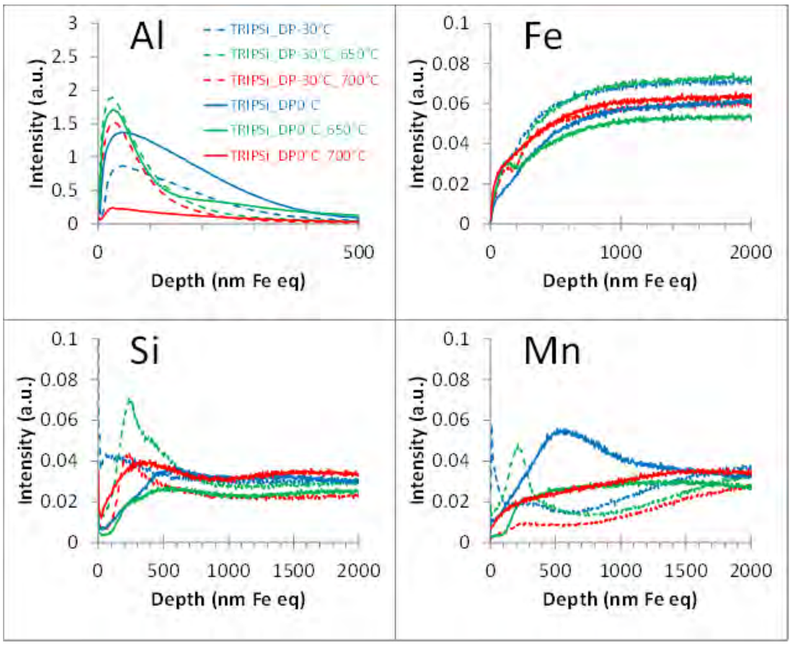

Figure 24: GDOS profiles after electrochemical dissolution of the zinc layer made on the galvanized TRIP-Si with/without an oxidation step and with/without water vapour injection.

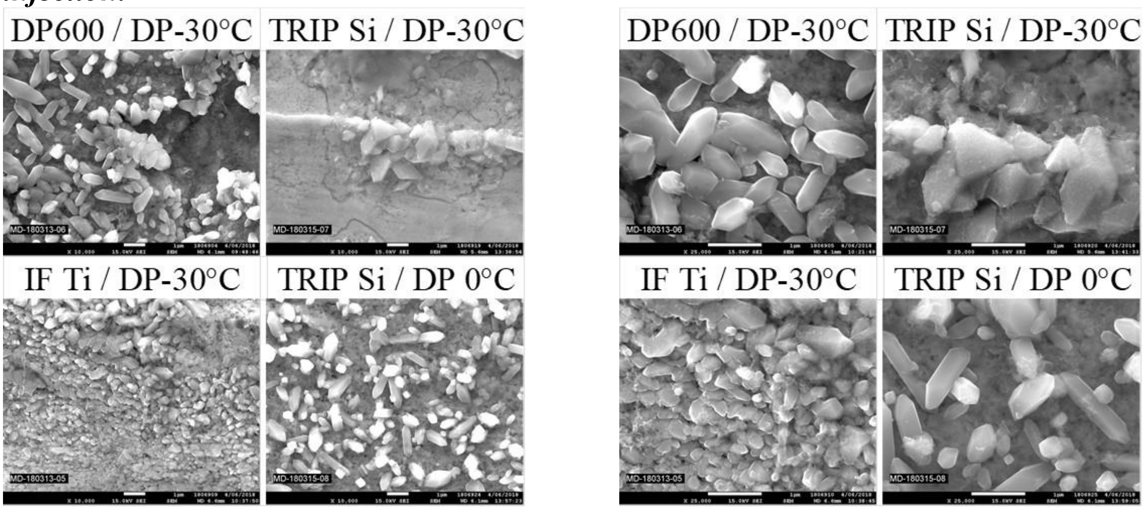

Figure 25: SEM images of the inhibition layer after electrochemical dissolution of the zinc layer: a more dense inhibition layer is observed on the IF Ti steel grade, but a clear improvement is also noticed at higher dew point on the TRI-Si steel.

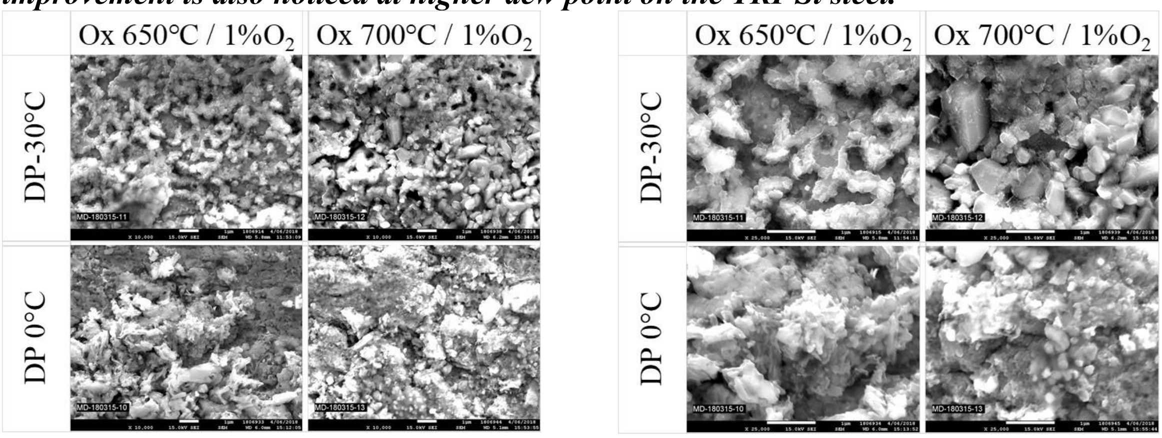

Figure 26: SEM images of the inhibition layer after electrochemical dissolution of the zinc layer: unusual pictures are obtained on the TRI-Si steel.

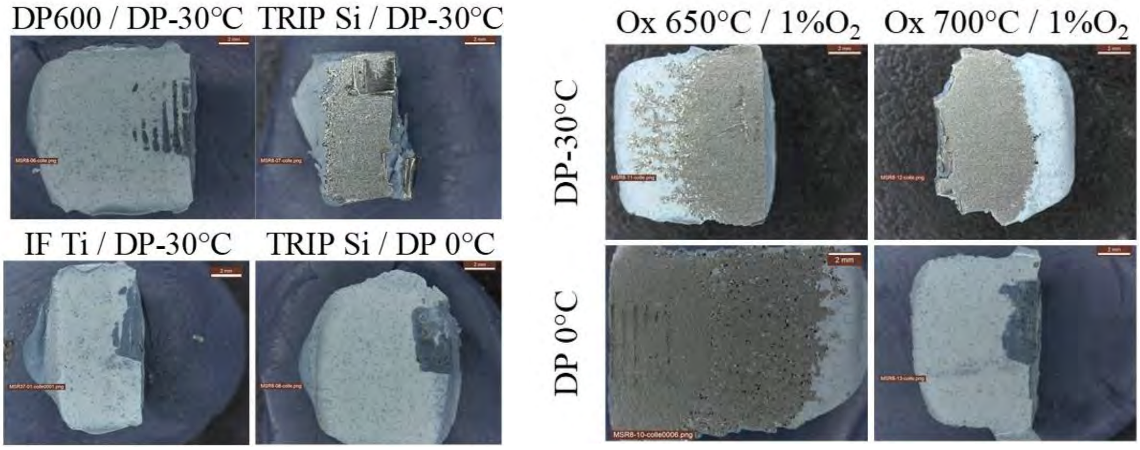

Figure 27: The bad coating adhesion is correlated with the presence of an important Mn/Si selective oxidation layer behind the inhibition layer.

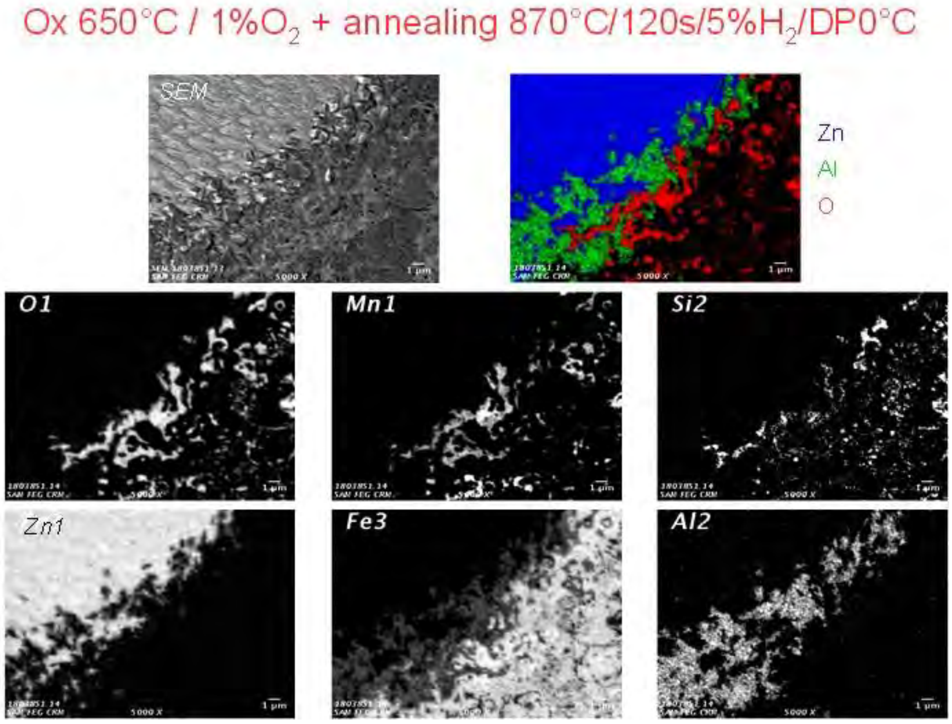

Figure 28: Auger mapping shows the presence of an intense selective oxidation behind the inhibition layer after annealing at high dew point and with an oxidation step at 650°C/3s/1%O_2 and hot dip galvanizing.

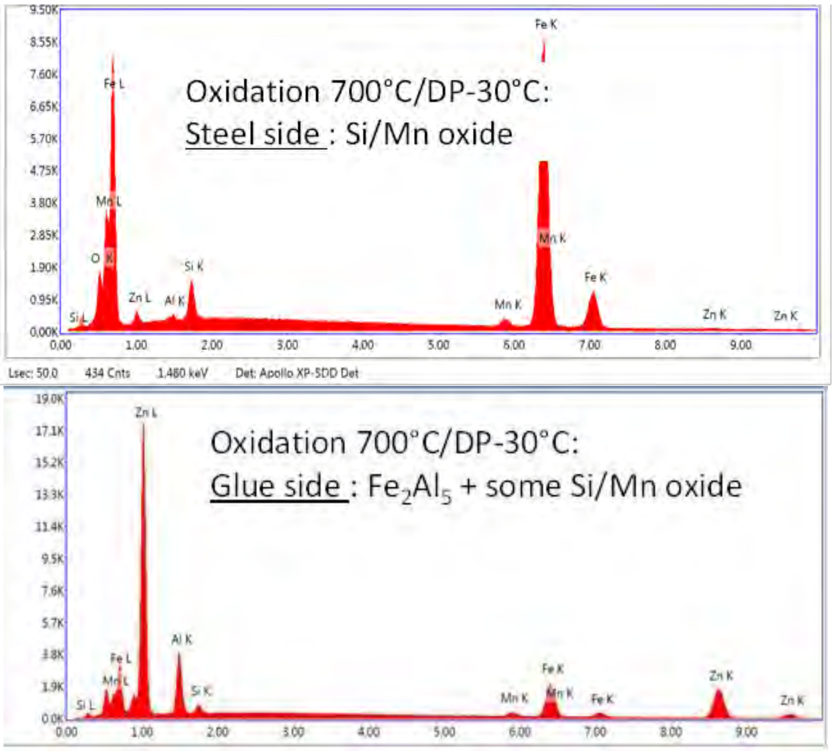

Figure 29: SEM-EDX analyses shows that the failure is located at the Si/Mn oxide layer interface.

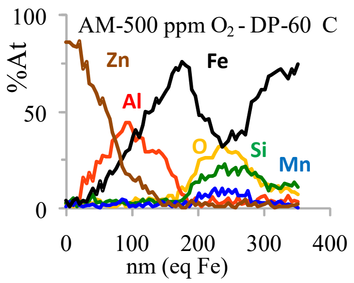

Figure 30: Auger analysis indicates that a thin (<100nm) Si/Mn segregation at the Fe_2Al_5/steel interface is at the origin of the bad coating adhesion (study ZCO54).

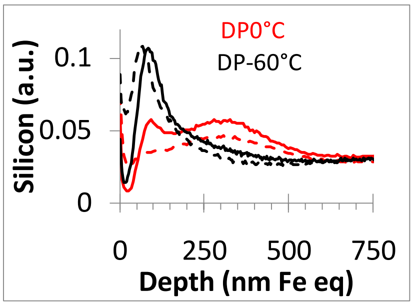

Figure 31: High dew point during annealing in oxidation conditions allows transferring Silicon oxidation to the internal mode.

4.3 Conclusion for the GI bath:

A correct coating appearance can already be obtained after standard annealing conditions (800°C/60s/5%H_2/DP-30°C) on the IF Ti, DP600 and DP980. This indicates that the external selective oxidation does not form a continuous layer, which allows the formation of a sufficiently continuous inhibition layer. The associated coating adhesion is always correct whatever the annealing conditions.
The annealing performed at high dew point, allows however enhancing zinc wetting and making a more continuous inhibition layer, which should improve the process robustness.
Finally, an oxidation step at 650°C-700°C/3s/1%O_2, further improves zinc wetting and the inhibition layer, without deteriorating the coating adhesion.

In the case of the TRIP Si steel, annealed with a Q&P thermal cycle (870°C/120s) before hot dipping, a correct zinc wetting and coating adhesion can only be obtained with an annealing at high dew point (5%H_2/DP0°C), without any oxidation step during heating.
Indeed, in classical atmosphere (5%H_2/DP-30°C) the zinc wetting and coating appearance are poor. If an oxidation step, performed between 650°C and 750°C, is introduced in the annealing cycle, zinc wetting is strongly improved but coating adhesion becomes unacceptable. This is due to the presence of a Si/Mn oxide at the steel / Fe_2Al_5 layer.

5. *Coatability with the ZM 11/11 bath*

5.1 Reactivity after annealing in reference condition:

The same wetting trials have been performed with a bath containing 1.1%Al and 1.1%Mg.

It has to be remembered that higher Mn external selective oxidation is noticed for the DP980, but in the same range than for the DP600 for Cr after annealing at 800°C / 60s (Figure 32). The Mn peak indicates a more homogeneous repartition of the Mn selective oxidation on the surface (higher intensity of the peak), associated with finer crystals (narrow peak). The Cr peak seems indicating that between these crystals, we can find bigger Cr(Mn) crystals (larger peak). The higher Mn amount in the DP980 steel (2.3wt%) in comparison with the DP600 (1.7wt%) could explain this selective oxidation difference.
Higher Si selective oxidation for the TRIP Si annealed at 870°C / 120s. Here again, the thin and intense Si peak on the top surface indicates a high coverage of a thin SiO_2 layer with bigger Mn/Si crystals (large Mn/Si peaks) inside this layer.

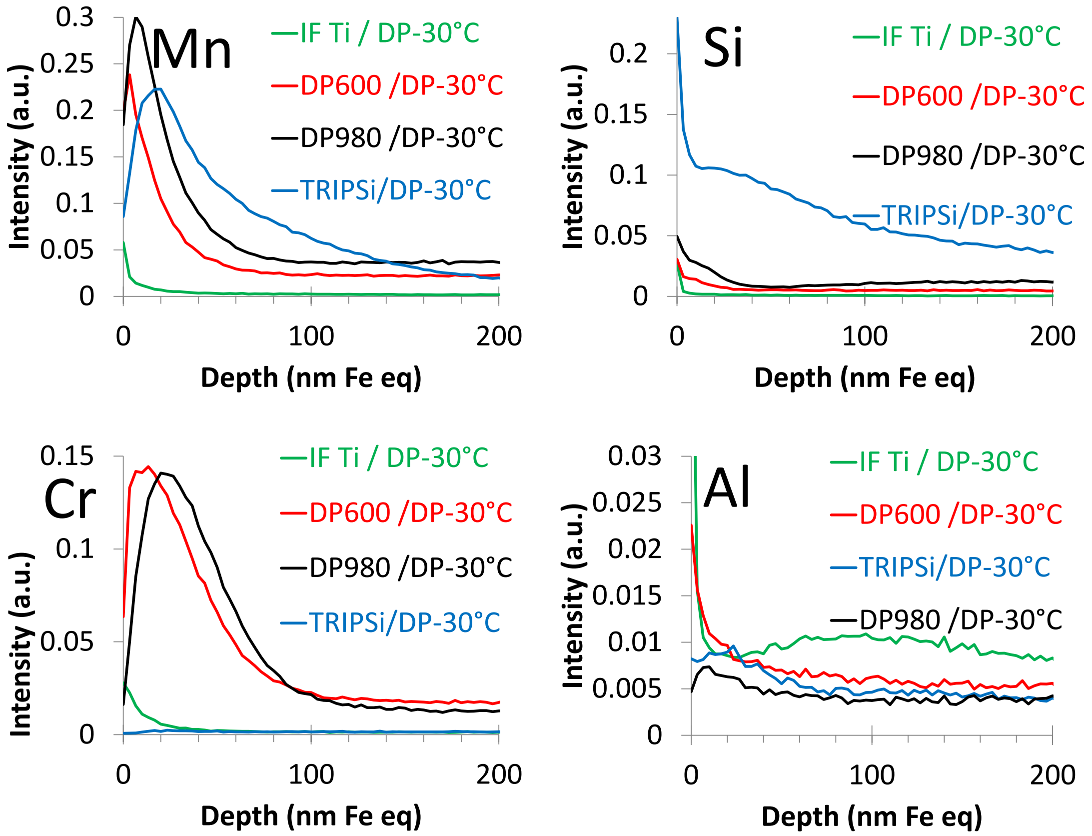

Figure 32: GDOS indicates Mn/Cr/Si external selective oxidation after standard annealing conditions (5%H_2/DP-30°C).

After annealing in this reference conditions (5%H_2/DP-30°C) the coating appearance and its adhesion where good for the IF Ti and the DP600 steel grades (Figure 33). The full panel size (100 x 200 mm) is scan on this picture.
The coated area for the DP600 is however lower than for the IF Ti steel. Indeed, the red line indicates that the bath wets a higher level for the IF Ti. Figure 34 illustrates that in the case of a good wetting, the bath fountain can reach higher levels according to the wetting behaviour.

If no bare spots are however visible on the DP600 panels, some are present on the DP980 grade, but their number and area are much more important for the TRIP-Si steel.

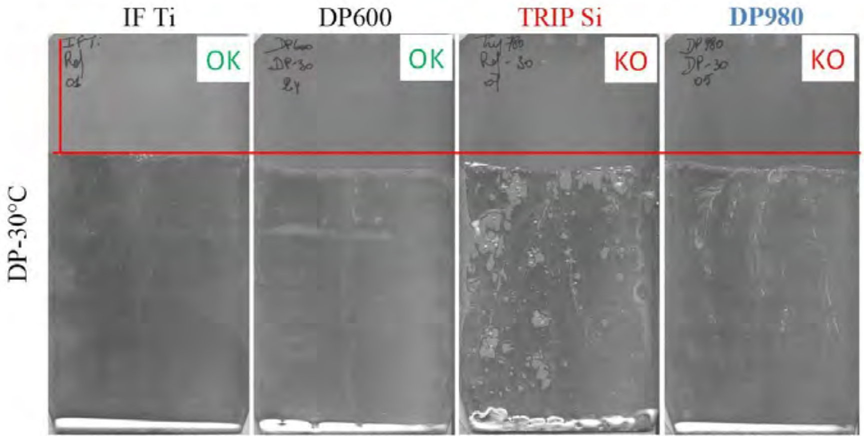

Figure 33: Pictures of the galvanized panels in the ZM 11/11 bath at 440°C after annealing in the reference conditions: 5%H_2/DP-30°C.
OK indicates a good coating adhesion and KO a poor one with coating delamination

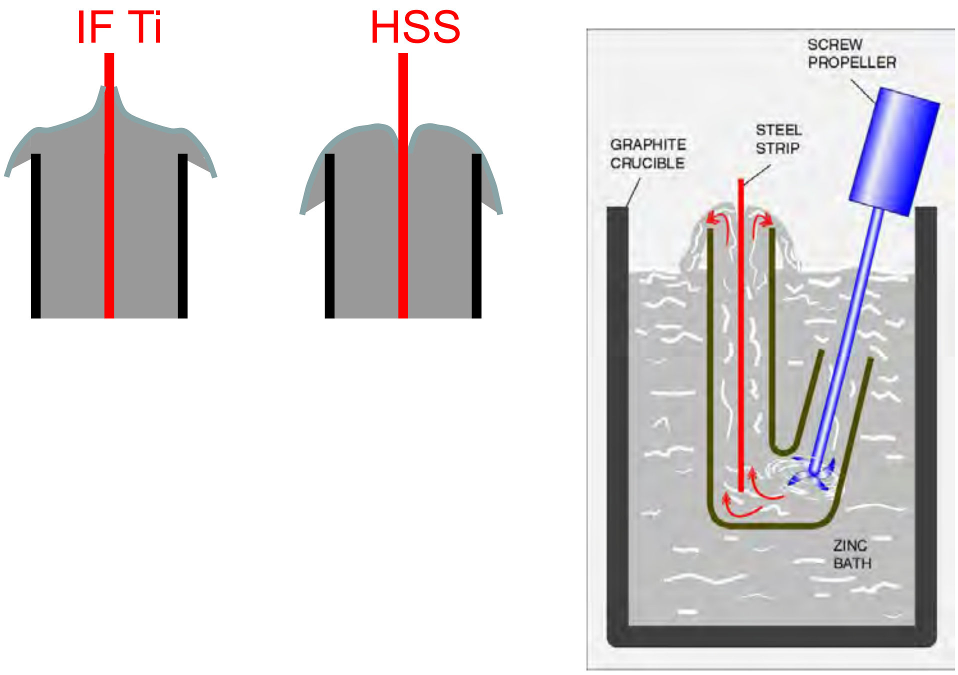

Figure 34: Good wetting induces more important zinc coverage on the panel.

Some oxide flows are also observed on some panel (mainly DP980). Figure 35 tries proposing an explanation of this behaviour. In case of a good wetting (IF Ti), oxide particles are rejected from the steel surface and they are then drag out of the sample during wiping.
In the case of insufficient wetting, these Al/Mg oxides could be trapped close to the samples and could stick on the panel when it comes out of the bath and flow then from top to bottom during wiping, which induces the formation of the visual pattern reported in Figure 33 and Figure 35.

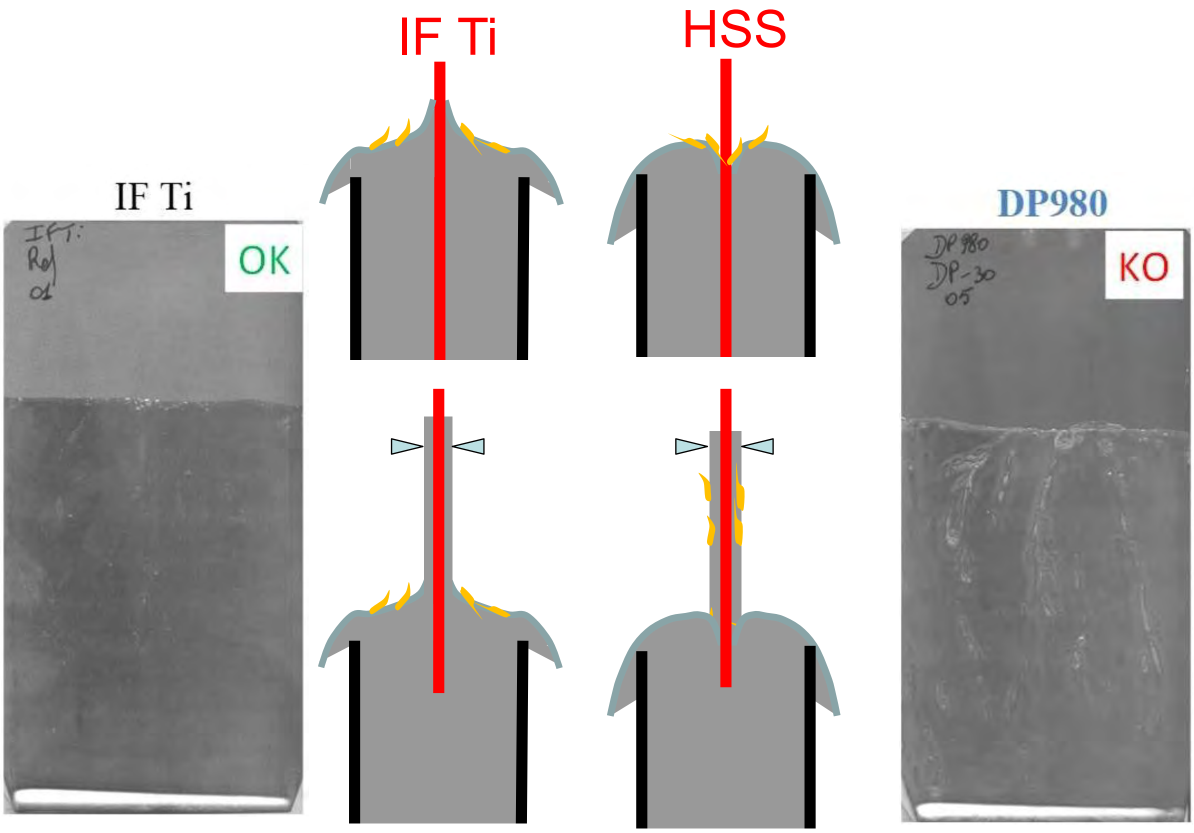

Figure 35: Good wetting helps repulsing the oxides covering the surface.

As previously discussed, the adhesion is tested after the application of a glue followed by a 90° bending. Figure 36 represents the glue side after the bending test. For the IF-Ti steel, the coating sticks on the sample. A complete coating delamination is observed for the TRIP-Si. After a classical annealing, the visual aspect and the adhesion are associated because they only depend on the reactivity during dipping.

This reactivity can be characterized by a GDOS profile of the Al signal, made after the coating removal by electrochemical dissolution. The GDOS profile of the ZM 11/11 inhibition layer indicates that the poor adhesion of the TRIP-Si is associated with a poor inhibition layer (Figure 37). The good adhesion of the IF-Ti is associated with a narrower and higher Al profile, which can be interpreted by thin crystals (narrow peak) with and homogeneous repartition (higher peak).

The DP980 steel should be covered with bigger Fe_2Al_5 crystals (large peak), which is probably due to the presence of a more continuous Mn(Cr) oxide layer before dipping. The non-homogeneous shape of the Al peak for the DP600 seems to indicate some small Fe_2Al_5 crystals between larger ones and remaining selective oxidation.

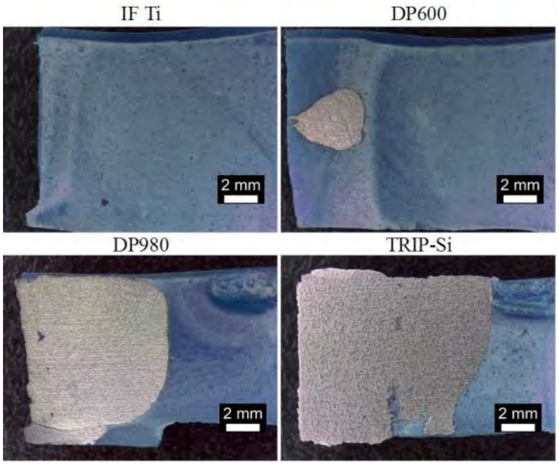

Figure 36: Picture of the glue side after bending: Decrease of the coating adhesion from the IF-Ti to the TRIP-Si after standard annealing (5%H_2/DP-30ºC).

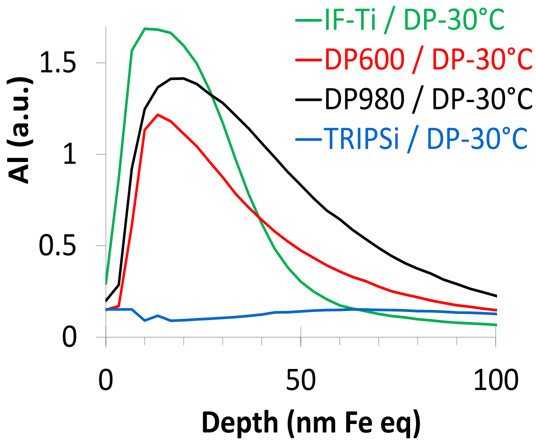

Figure 37: GDOS Al profile corresponding to the inhibition layer after having removed the coating (after standard annealing 5%H_2/DP-30ºC).

The SEM observation of the ZM 11/11 inhibition layer (Figure 38) indeed indicates fine Fe_2Al_5 crystals homogeneously split over the surface. No inhibition layer is observed for the TRIP-Si. The Fe_2Al_5 crystals are bigger for the DP980 with numerous holes between them. The selective oxidation, which was in these holes, has been dissolved during the zinc etching process. A more continuous inhibition layer is observed for the DP600 steel grade. The size of the Fe_2Al_5 crystals is larger than the one observed for the IF-Ti but smaller than in the case of the DP980. This SEM pictures confirms the previous GDOS analyses.
Therefore, the reactive wetting should be better for the IF-Ti grade and progressively deteriorated respectively for the DP600, the DP980 and the TRIP-Si.

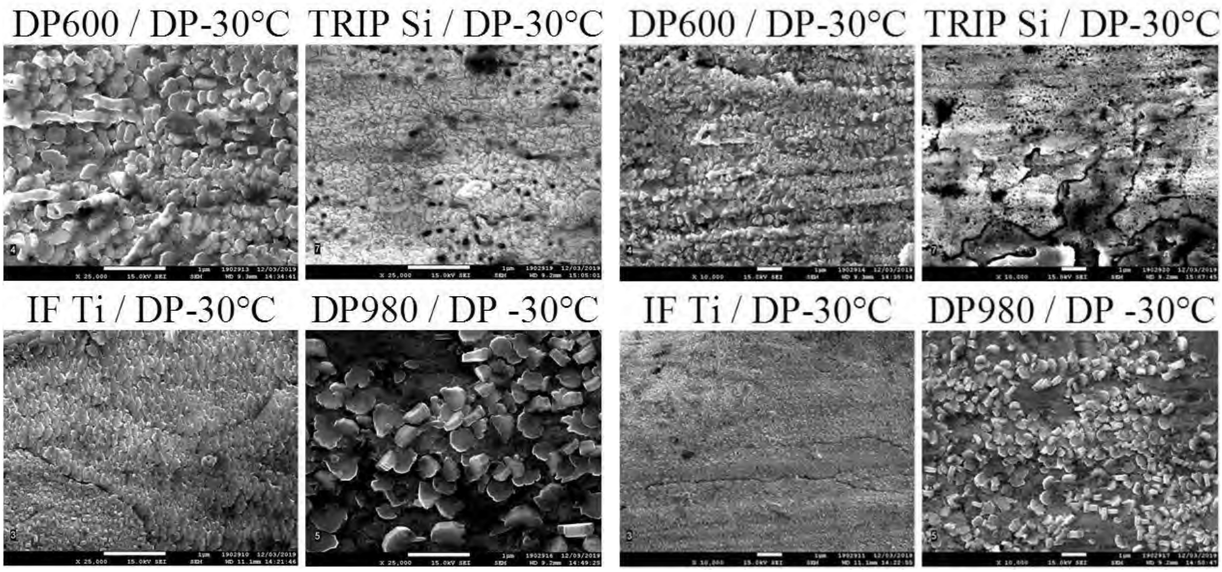

Figure 38: SEM images of the inhibition layer after electrochemical dissolution of the zinc layer.

In parallel, the wetting measurements, made with the sessile drop method (Figure 39), indicates that the wetting behaviour of the DP600 and the DP980 steels are in the same range (90°-100°), which is the maximum acceptable limit. Only the IF Ti shows a significantly better wetting, which is consistent with the wetting observations made on the hot dipped panels. The wettability, measured with the TRIP-Si steel, is clearly worse than for the DP600, which is again in line with observations made on the panels of Figure 33.

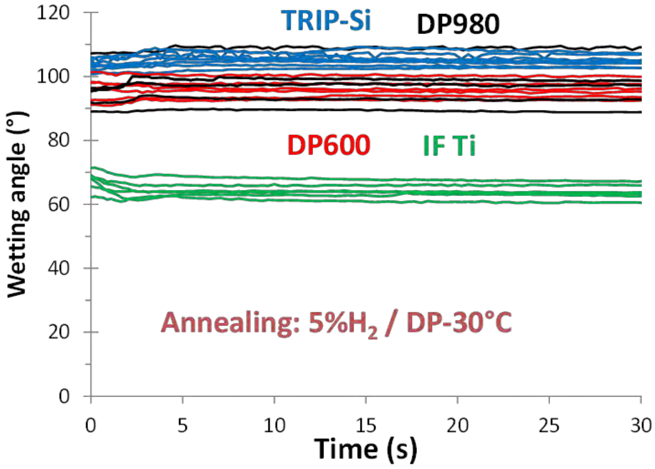

Figure 39: The TRIP-Si steel has a poorer wetting behavior after annealing in standard conditions than the DP980.

It has also to be noticed that the zinc spreading is very different of the one obtained for the classical GI bath (Figure 20) after the same annealing conditions.

This difference is attributed to the destabilization of the Fe_2Al_5 layer with time in the case of the GI droplet, which induces a strong Fe-Zn reactivity. A higher Al amount in the ZM 11/11 droplet allows keeping a stable Fe_2Al_5 layer.

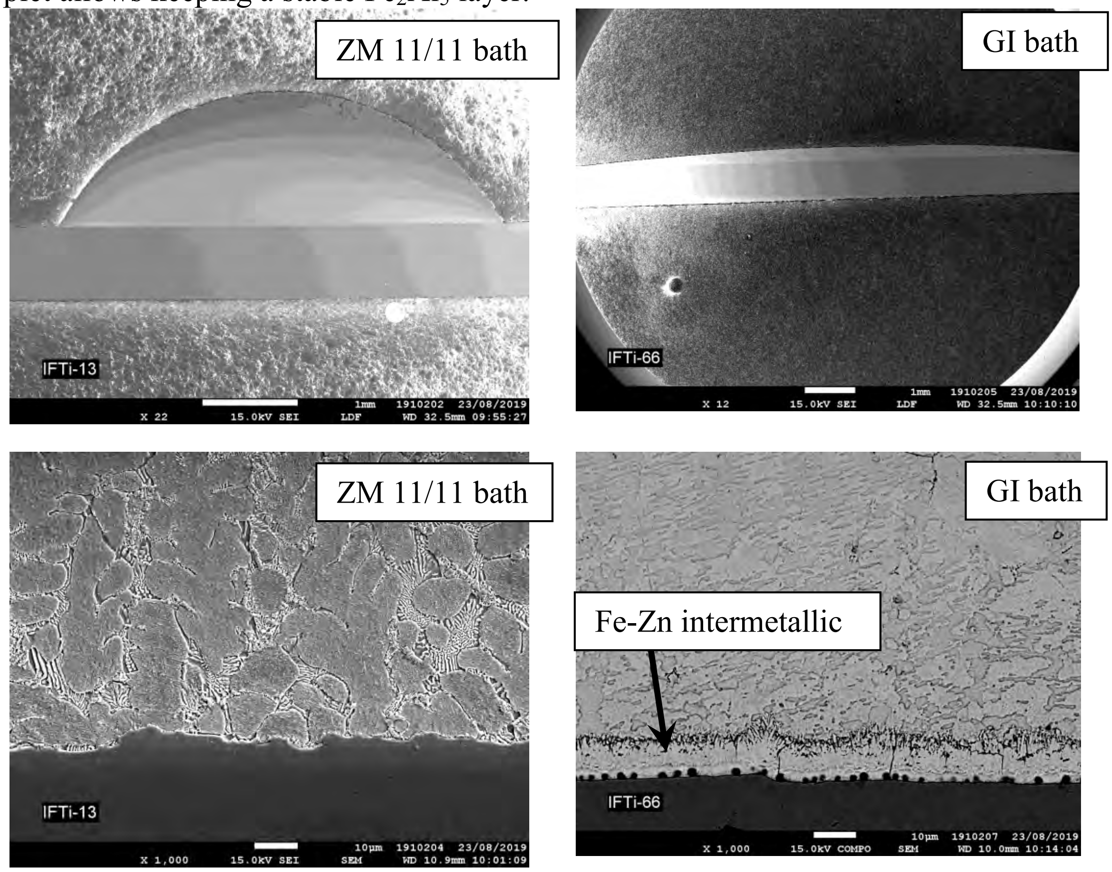

Figure 40: Cross section made through a GI or a ZM 11/11 droplet after 30s of contact with an IF-Ti steel grade.

It is also possible that Al/Mg oxide around the liquid droplet before it touches the steel surface, can block further reactivity and zinc spreading. The same behaviour was noticed during dipping in a GI bath by increasing the dew point during the wetting measurements with a meniscograph apparatus (Figure 41), which also induces an increase of the Al oxide thickness and strongly reduces spreading.
Figure 42 also shows that Mg additions can significantly improve zinc wetting. This observation is probably due to the mechanical properties of the Mg oxide, which must be less ductile than the Al oxide. The Mg increase, will induce a replacement of the Al oxide by the less detrimental Mg oxide.
Therefore, it is important to always control the dew point around the droplet in restricted range (-62°C<DP<-58°C) to allow comparing the different measurements.

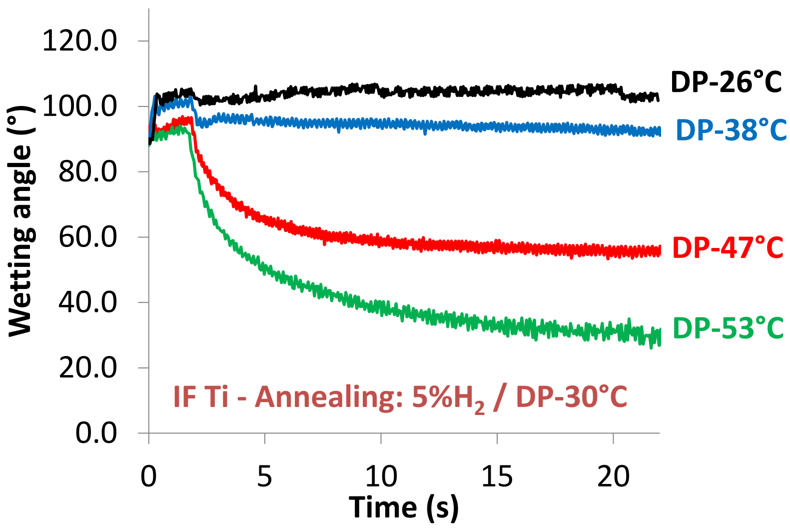

Figure 41: Wetting evolution in a Zn-0.2%Al bath measured with a meniscograph apparatus.

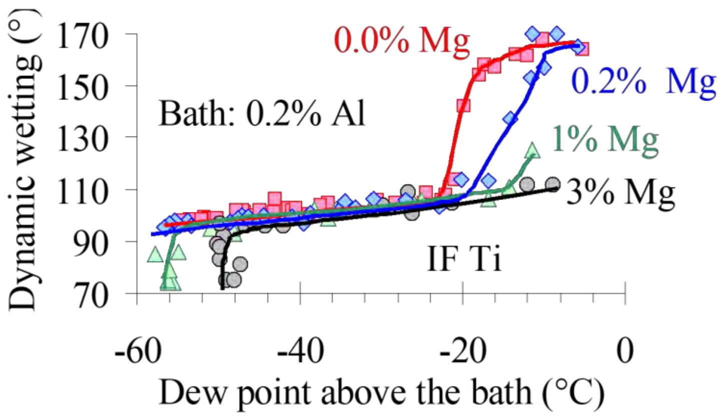

Figure 42: Mg addition in the GI bath improves wetting.

5.2 <u>Reactivity after annealing at high dew point:</u>

The external selective oxidation significantly decreases when the annealing is made at high dew point (Figure 43). A finer external layer containing mainly Mn oxides are however still present on the top surface.

The more intense Mn peak noticed for the DP980 steel seems indicating that small Mn oxide crystals still cover an important part of the grain boundaries and the surface, even after annealing at high dew point.
The steel decarburizing thickness increases up to around 35µm – 40µm. The behavior of the DP980 steel grade is different from the other steel grades because no complete decarburizing is noticed. It is probably due to an insufficient soaking temperature, which does not allow a complete dissolution of the carbides. Indeed, this steel grade contains Nb/Ti carbides, which dissolution is more difficult at 800°C.

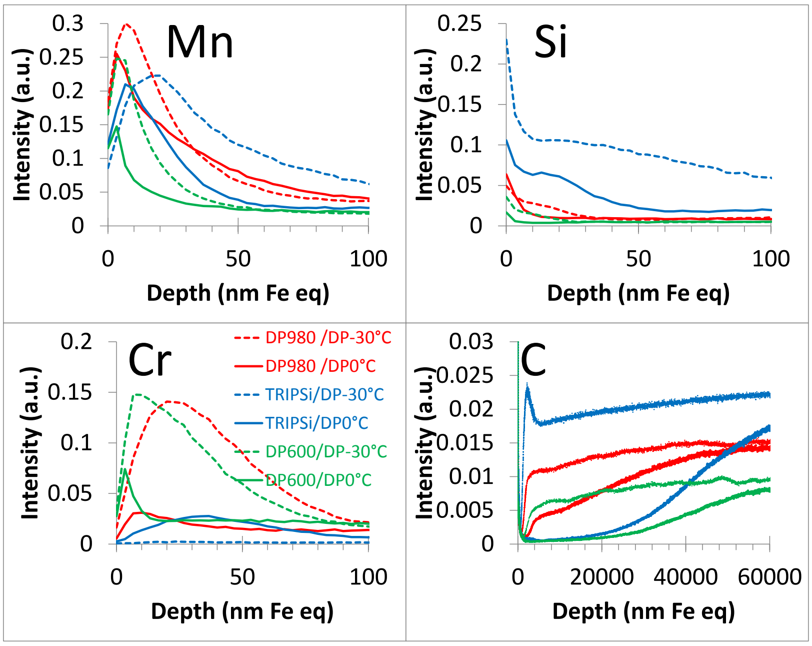

Figure 43: Significant decrease of the external selective oxidation after annealing at high dew point.

If we focus on the DP600 steel, it can be seen that the annealing, made at high dew point, significantly improves the zinc height for the DP600 panel (Figure 44), while being still lower than for the IF-Ti panel, which should indicate a better bath wetting. This visual observation is confirmed by the wetting measurements reported in Figure 45.

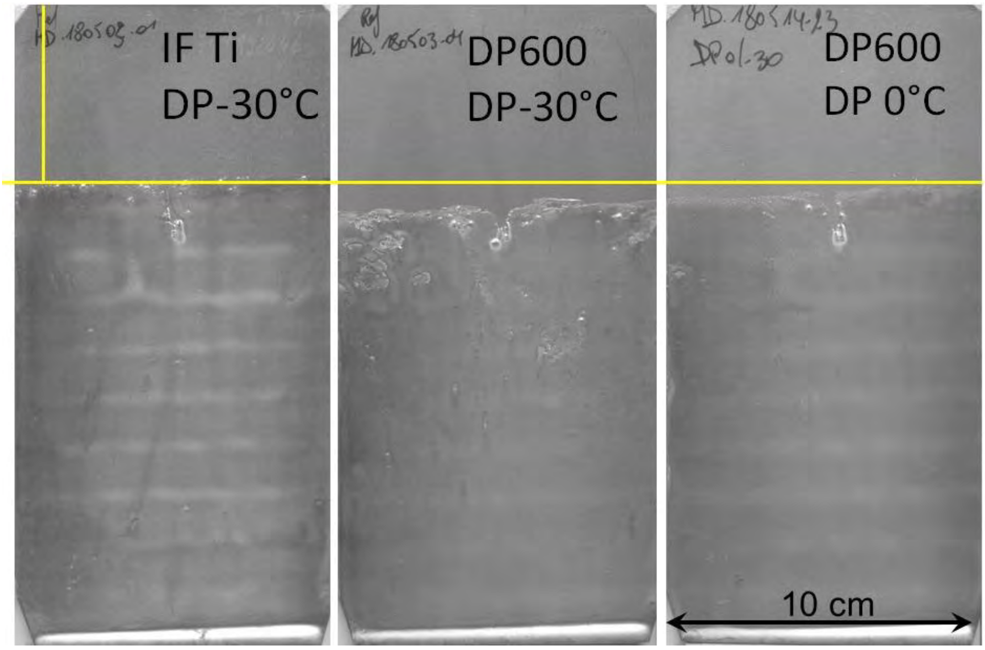

Figure 44: Wetting is improved on DP600 steel grade after annealing at high dew point → Confirmed by wetting measurement.

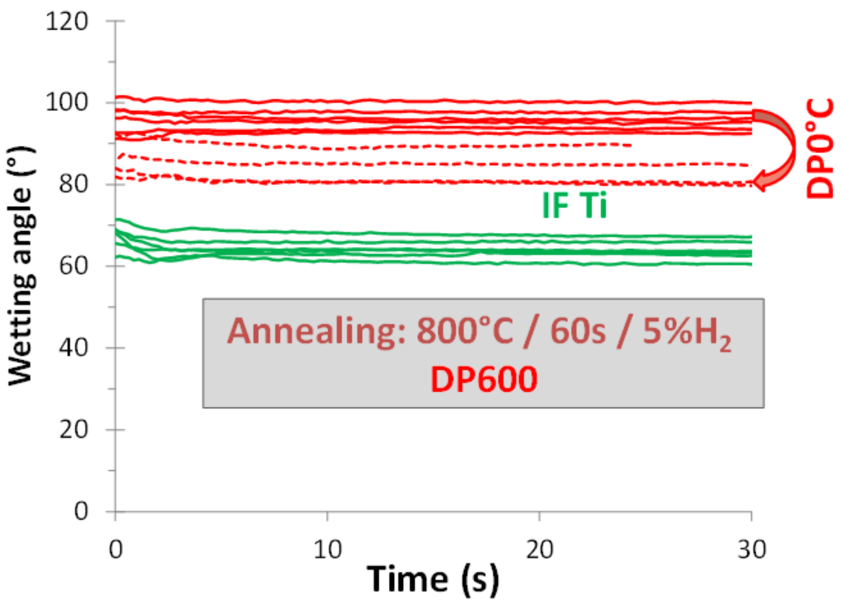

Figure 45: A significant wetting improvement is also measured for the DP600 steel grade after annealing at high dew point.

The most interesting information is however the improvement of the coating appearance and adhesion noticed for the TRIP-Si steel after an annealing at high dew point (Figure 46). Some improvement of the coating adhesion can also be noticed for the DP980 after annealing at high dew point.
The flow of the Al/Mg oxides on the panel indicates that the wetting is always critical.

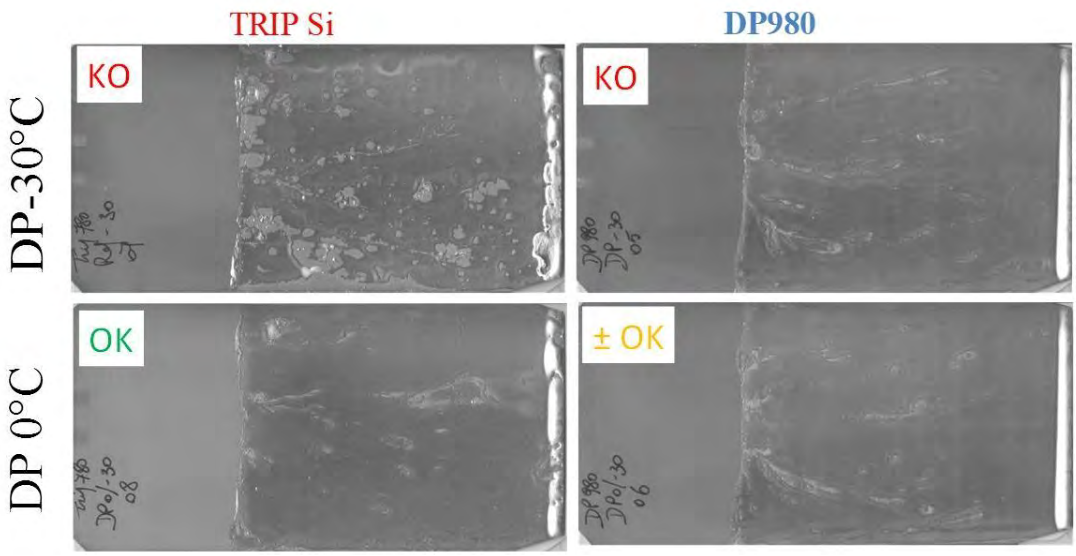

Figure 46: The coating appearance and adhesion are improved for the TRIP-Si after annealing at higher dew point. Quite no improvement is noticed for the DP980 (OK=good adhesion and KO = bad adhesion).

As discussed on the previous slide, Figure 47 illustrates the significant improvement of the coating adhesion after an annealing at high dew point. This improvement is however weaker for the DP980 steel. This is probably due to the higher amount of Mn (Si) residual oxides.

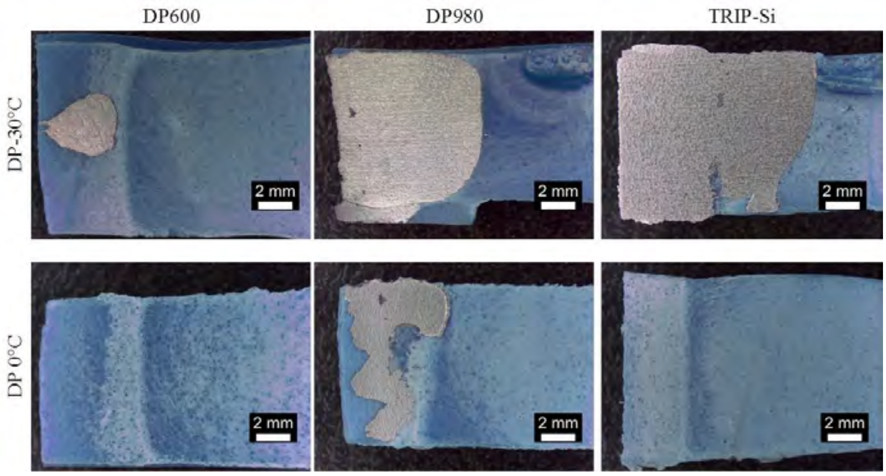

Figure 47: Picture of the glue side after bending: Improvement of the coating adhesion after an annealing at high dew point.

The correlation between the GDOS profile for the inhibition layer (Figure 48) and the coating adhesion is however difficult for the DP980 steel. Indeed, for the TRIP-Si steel, it is clear that the annealing at high dew point has partly allowed a transfer from the external oxidation to the internal mode, which has permitted the formation of a sufficient inhibition layer and consequently a correct adhesion.

For the DP980, it seems that the transfer from the external to the internal oxidation was not sufficient to change the formation of the inhibition layer, even if this graph indicates that the coverage of the surface by the inhibition layer should be more important for the DP980 steel than for the TRIP-Si steel.

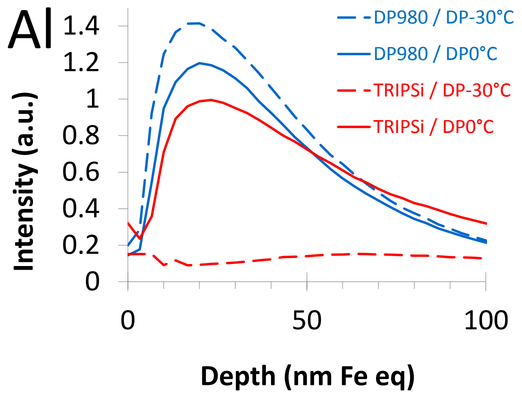

Figure 48:Significant increase of the Al peak for the TRIP-Si in the GDOS profile indicates the formation of a correct inhibition layer.

The SEM images indeed show a much better surface coverage with Fe_2Al_5 crystals. Even if the Fe_2Al_5 crystals are far from covering 100% of the surface, the crystals repartition is relatively continuous over the surface, which means than zinc bridges are able to finally make a continuous coating coverage.

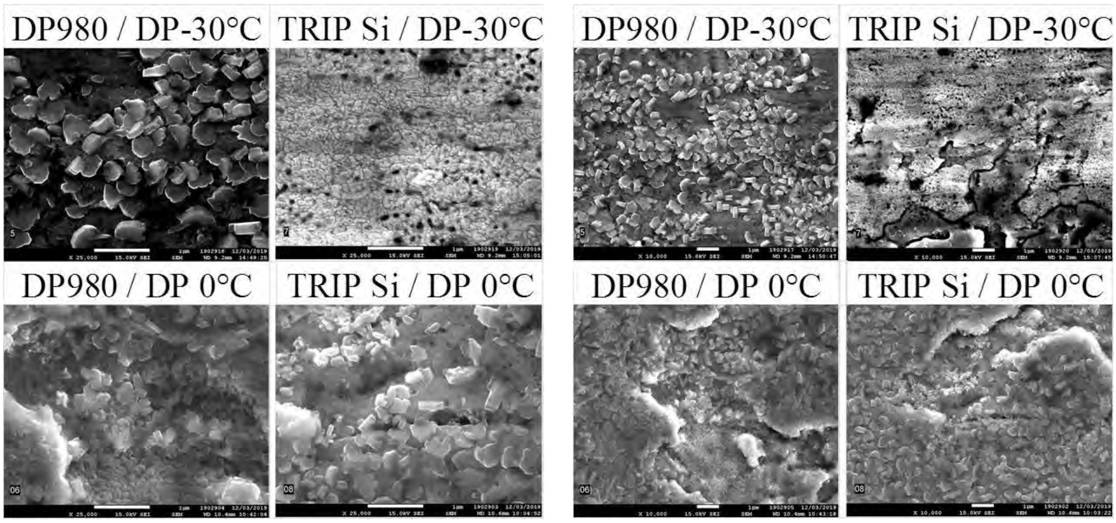

Figure 49: SEM images of the inhibition layer after electrochemical dissolution of the zinc layer: a better coverage is obtained after annealing at high dew point.

The wetting measurements, reported in Figure 50, confirm that a wetting angle between 80° and 95° is obtained for the TRIP Si, which is still an acceptable range for a correct coating appearance (it is better than for the reference DP600 steel grade). Surprisingly, the wetting improvement for the DP980 is weaker (range between 90° and 100°), which however confirms the less significant improvement of the coating adhesion and coating appearance with water vapour injection for the DP980. This is probably explained by the higher Mn oxide coverage at high dew point (Figure 43 and Figure 51).

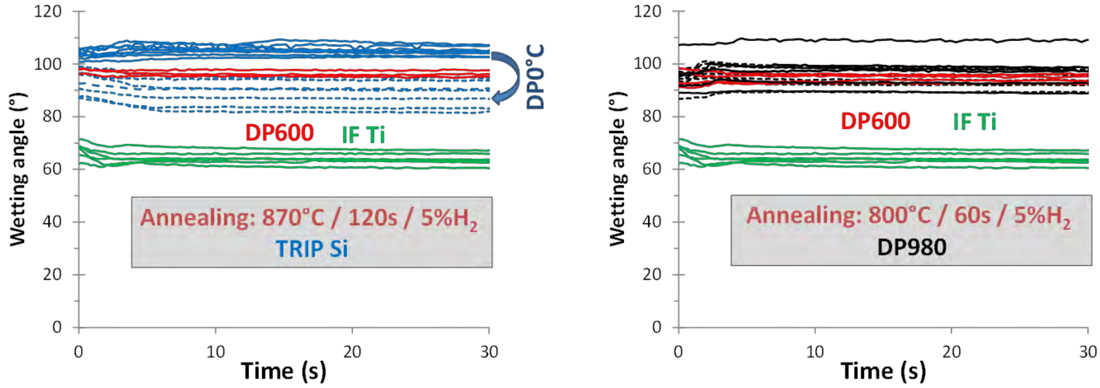

Figure 50: The wetting improvement after an annealing at high dew point (dot lines) is more notable on the TRIP-Si steel than for the DP980.

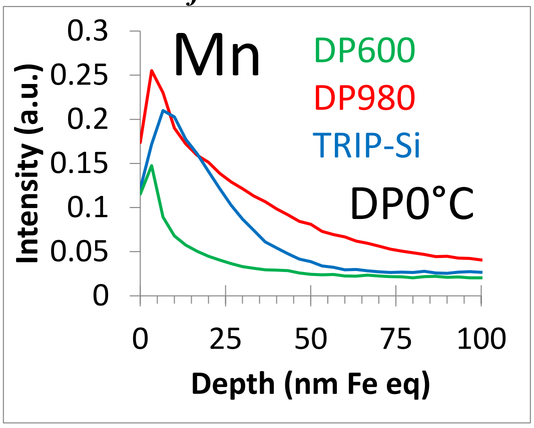

Figure 51: GDOS profile shows a higher surface coverage by a thin Mn oxide for the DP980.

5.3 Reactivity after an oxidation / reduction process:

5.3.1. Study for the TRIP-Si steel

If an oxidation step is introduced during heating, the iron reduced layer on the TRIP-Si is kept after the full annealing cycle, even after a soaking of 2 minutes at high temperature (870°C), with however some holes covered with Mn/Si oxides (Figure 52).

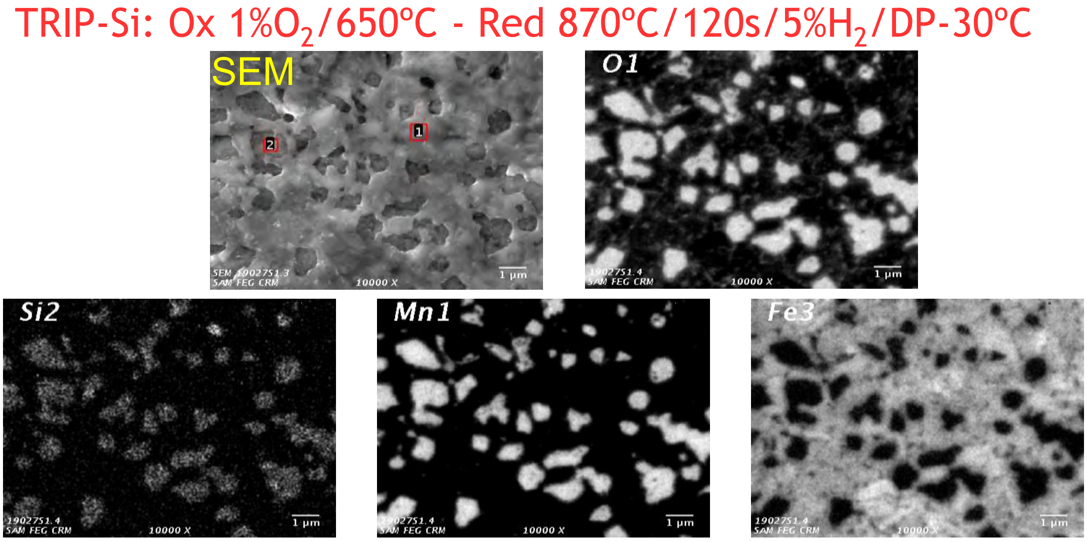

% at	O	Si	Mn	Fe
point 1	6.9	2.0	8.8	82.3
point 2	40.4	17.3	36.3	6.0

Figure 52: Auger analyses on the top surface indicate holes in the reduced iron layer

The oxidation / reduction process, associated with a soaking at low or high dew point, always gives a very significant improvement of the coating appearance for the TRIP Si steel grades (Figure 53). The improvement increases for higher oxidation temperatures and after soaking at high dew point.

The coating adhesion is however always poor.

As in the case of the GI bath, it can be supposed that this bad adhesion is due to the presence of a weak Si/Mn oxide at the steel / inhibition layer interface.

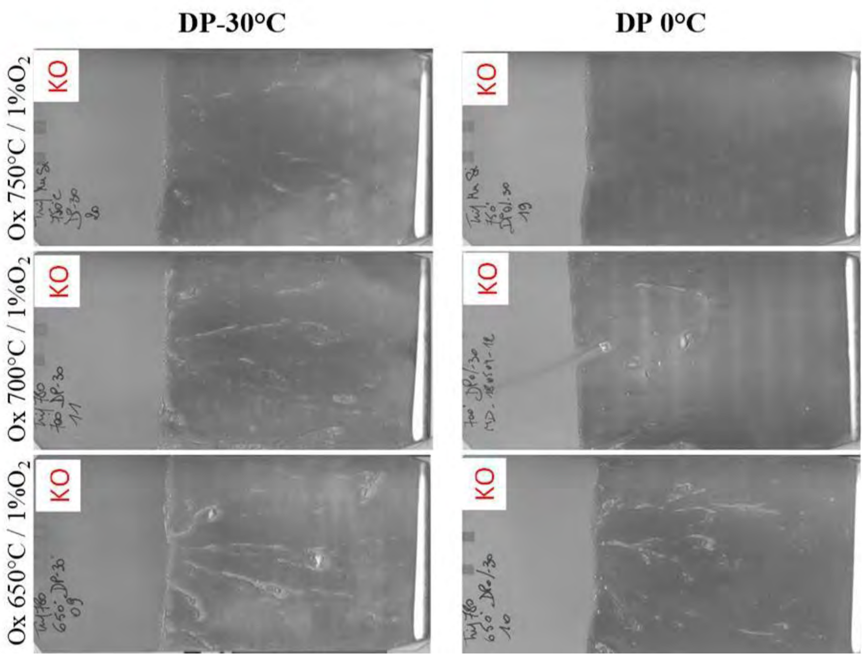

Figure 53: Nice TRIP-Si panels can be obtained after pre-oxidation but coating adhesion is always very poor.

SEM-EDX analyses made after the adhesion test on the Glue side and the corresponding steel side had clearly shown that the coating delamination observed after the bending test on a GI coating is located around the Si/Mn oxide (Figure 29).

This Mn-Si selective oxidation at the steel/reduced iron interface can also be observed by GDOS analyses after the complete annealing cycle for the TRIP-Si (Figure 54). The presence of metallic iron on the top surface with an oxidation step, especially if the soaking is made at high dew point, explains the nice coating appearance reported in Figure 53.
This figure also represents the glue side after the bending test. A complete coating delamination is observed for the TRIP-Si.

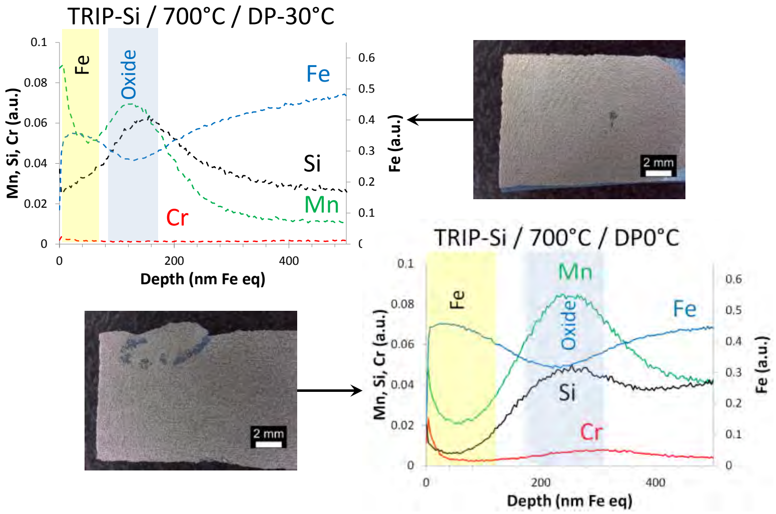

Figure 54: GDOS profile after the full annealing cycle showing Mn-Si segregation at the steel / reduced iron interface and corresponding coating delamination.

To better characterize the steel / coating interface, a maximum wiping (max N_2, low sample speed) was applied after hot dipping. Auger observations (Figure 55) indicate that some de-wetting areas can be observed between coating islets (point 1). The de-wetted areas are covered with Mg oxides. It is difficult to say if the MgO film was deposited on the coating before dipping or if it is formed after wiping in the protective atmosphere (selective oxidation mechanism), but the very thin inhibition layer (Al signal) seems however to indicate that the reactivity was not optimum. As no significant Mn and Si can be observed in the in depth profile, it could be imagine that the poor wetting is more associated with the deposition of a Mg oxide film before dipping.
On the areas covered with the coating, an inhibition layer is detected at the steel / coating interface with always some Si/Mn selective oxide behind. This confirms previous observations made with the GI bath (Figure 28).

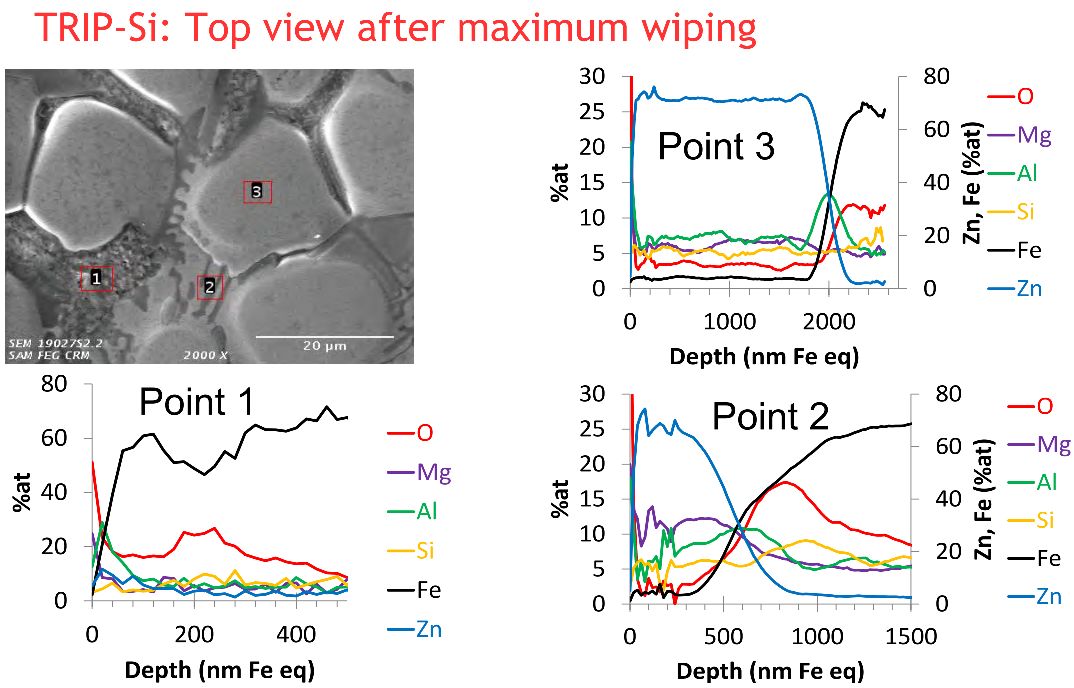

Figure 55: Auger analyses indicate the presence of oxide under the Fe_2Al_5 layer.

Auger mapping, made after having sputtered the coating from point 3 in Figure 56 confirms the presence of Mn/Si oxides behind the inhibition layer, which is probably responsible for the bad adhesion. This Fe_2Al_5 layer has been formed by the dissolution of the thin reduced iron layer covering the selective oxidation. No Mg oxide is detected at this interface to explain the coating delamination. Only metallic Mg is observed inside the zinc coating.

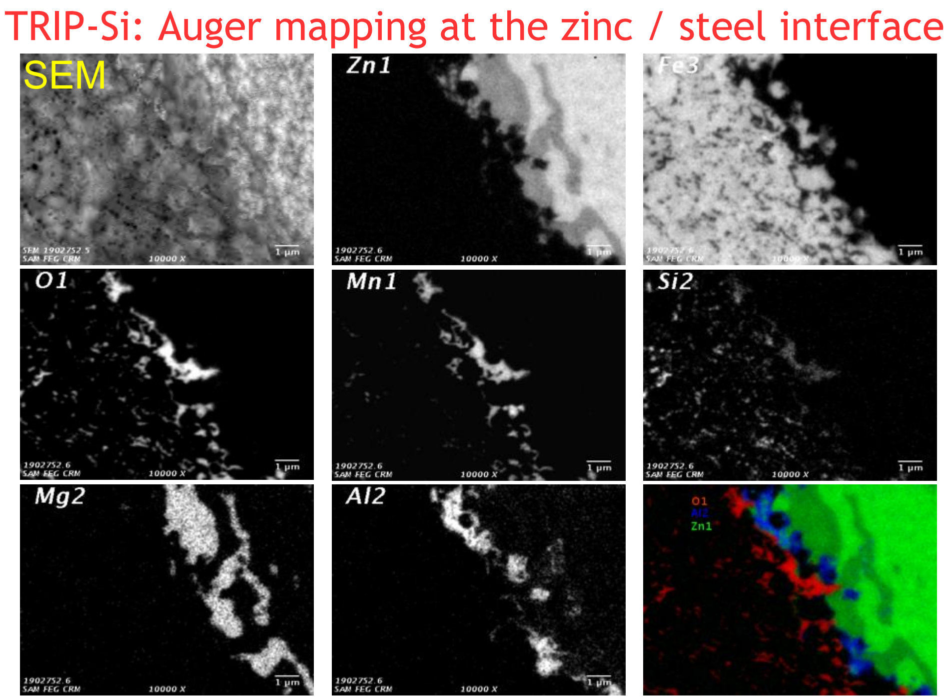

Figure 56: No oxidized Mg observed by Auger mapping under the Fe_2Al_5 layer, but only Mn-Si oxides.

The wetting measurements (Figure 57) confirm that a significant wetting improvement is measured after the ox/red process. The dew point during soaking has a weak influence on the wetting behaviour during the first 3 seconds. During this short delay, the oxidation temperature has also no significant influence if it is made between 650°C and 700°C. This comment is not exactly in agreement with the panel observation reported in Figure 53, which shows an improvement of the coating appearance after oxidation at higher temperature and for a higher dew point. This difference could be explained by the fact that the samples for the wetting measurements are cooled to room temperature after the oxidation step. It is not the case for the MultiDip panels. It could be imagine that a pollution can occur during the air exposure. Moreover a longer reheating in RTF atmosphere can also change surface preparation.
However, the general wetting behaviour also explain that a good coating appearance can be obtained because the wetting is close to the one measured for the IF-Ti steel after 3 seconds of contact.

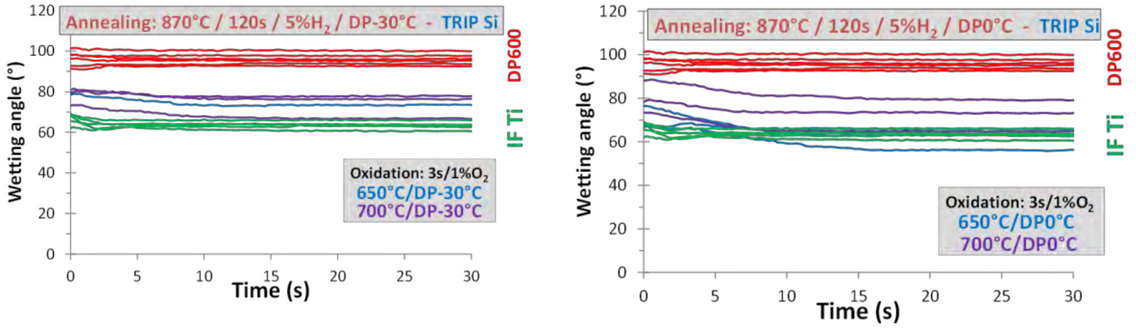

Figure 57: Wetting measurements confirm that an oxidation step improves the wetting behaviour of the TRIP-Si steel grade. The annealing at high dew point again gives an additional effect.

After hot dipping in the ZM 11/11 bath, the presence of a correct inhibition layer is in line with the wetting measurements and the coating appearance. The weaker intensity of the Al peak for the TRIP-Si in comparison with the one measured for the IF-Ti, indicates a lower coverage of the inhibition layer. A slightly better Al signal is measured at higher dew point, which is in good agreement with the coating appearance.

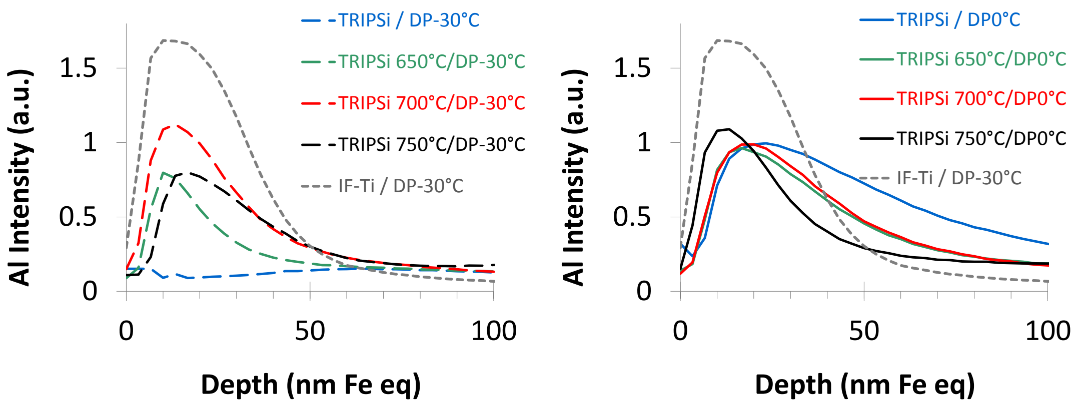

Figure 58: GDOS profile of the Al signal associated with the inhibition layer after hot dipping in the ZM 11/11 bath. The stronger Al peak at DP0°C is in line with the better wetting behaviour.

The aspect of the inhibition layer is very unusual. The high surface reactivity has induced the formation of very fine Fe_2Al_5 crystals, but significant areas without inhibition layer should indicate a former presence of selective oxidation, a lower Al peak in the GDOS profiles and a weaker wetting.

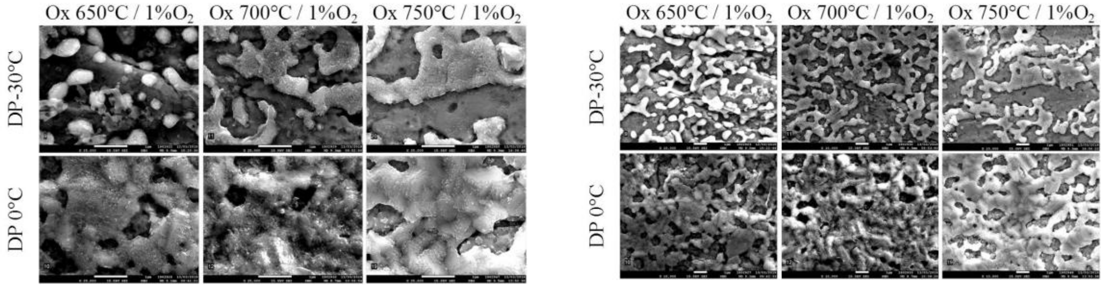

Figure 59: SEM images of the inhibition layer after electrochemical dissolution of the zinc layer.

To conclude, bad coating adhesion have been observed after an oxidation / reduction process, especially for the TRIP Si steel due to the presence of Mn/Si oxide film at the steel / reduced iron layer.
Therefore, some additional work has been made to try proposing new annealing conditions. Based on the idea that this bad adhesion was due to Si/Mn segregation at the steel / oxide interface, it was proposed to increase the dew point during the heating step to limit external silicon segregation before the oxidation step. An additional effect could be obtained by limiting the oxidation temperature and consequently the possible Si diffusion to the steel/iron oxide interface.

If a higher dew point doesn't give any coating adhesion improvement for the TRIP-Si, the decrease of the oxidation temperature to 600°C however brings a clear beneficial effect.

Further analyses are needed to explain this behaviour (oxide characterisation, surface composition before and after hot dipping).

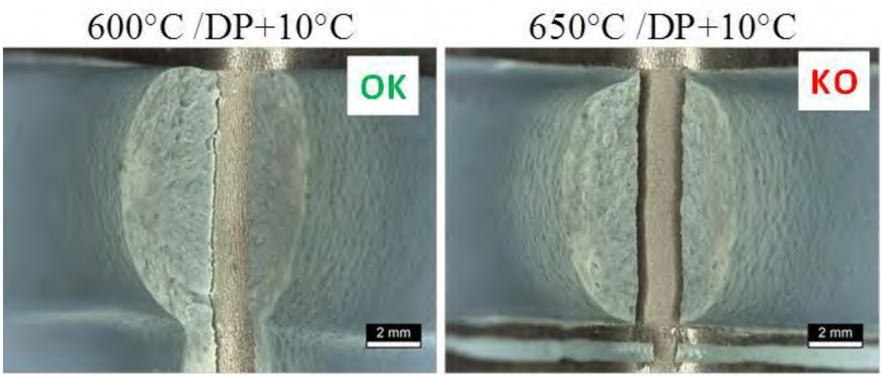

Figure 60: No influence of a higher dew point but much better coating adhesion at lower temperature for the TRIP-Si.

5.3.2. <u>Study for the DP980 steel</u>

Figure 61 shows the Auger analyses, made for the DP980 steel, after the complete annealing cycle. A more important Mn oxidation is formed along the steel grain boundaries. Again, Mn/Si oxides are not covered with the metallic iron layer.

DP980: Ox 1% O_2/650°C - Red 800°C/60s/5% H_2/DP0°C

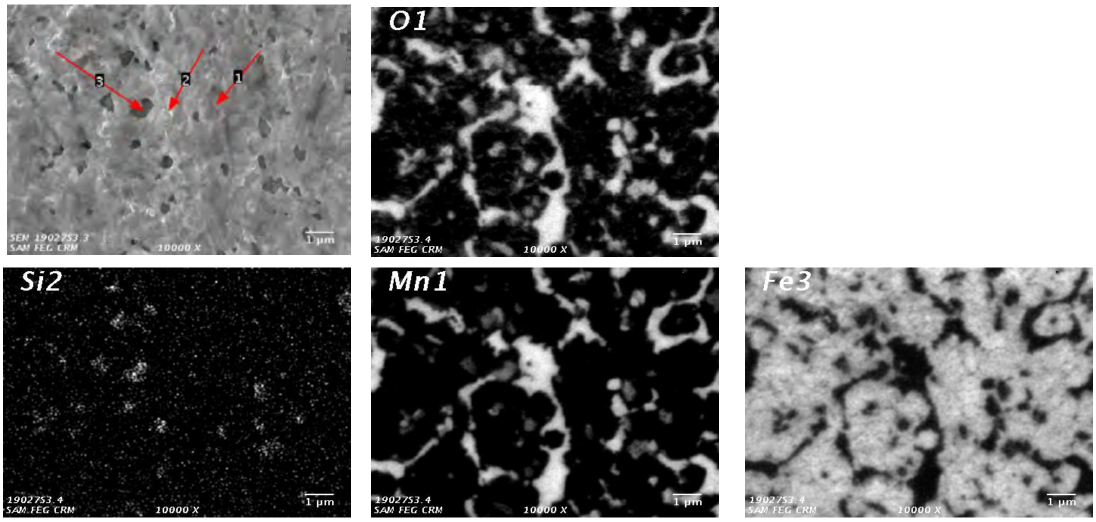

%at	O	Si	Mn	Fe
Point 1	12.7	0.0	0.0	87.3
Point 2	59.9	0.0	33.1	7.1
Point 3	52.0	8.2	22.9	16.9

Figure 61: DP980 - Auger mapping after the complete annealing cycle showing Mn oxide along grain boundaries.

It can be seen in Figure 62 that, after having sputtered the reduced iron layer, the visible iron grains size is in good agreement with the previous MnO repartition along grain boundaries. The thickness of these MnO is relatively important (± 80nm Fe equivalent).

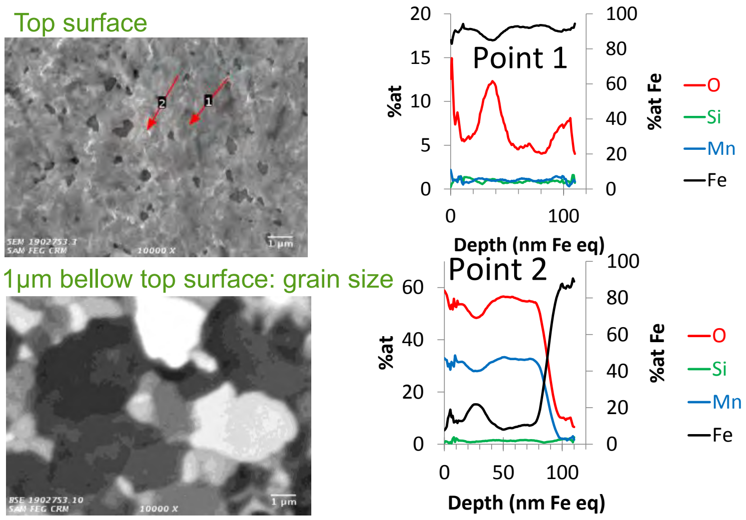

Figure 62: DP980 - Auger profile from the top surface after complete annealing: High thickness of the Mn oxides along grain boundaries.

After hot dipping, nice coating appearance and coating adhesion can also be obtained for DP980 panels but the understanding of the variation of the coating adhesion is more difficult (Figure 63). It can also be observed that, as it was the case for the TRIP Si, a better coating appearance is noticed for the more important oxidation condition (higher temperature and dew point).

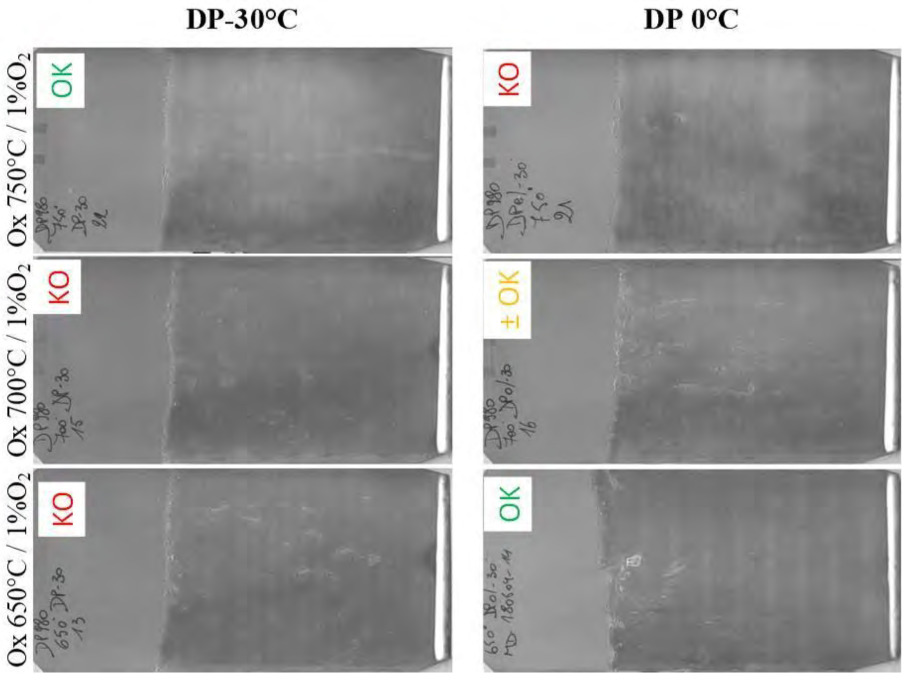

Figure 63: Nice coating appearance and coating adhesion can be obtained for DP980 panels.

Indeed, Figure 64 shows that the coating sticks sometime on the glue side, which indicates a bad adhesion but there is no correlation with the dew point or the oxidation temperature. GDOS and SEM analyses have been made to try proposing an explanation.

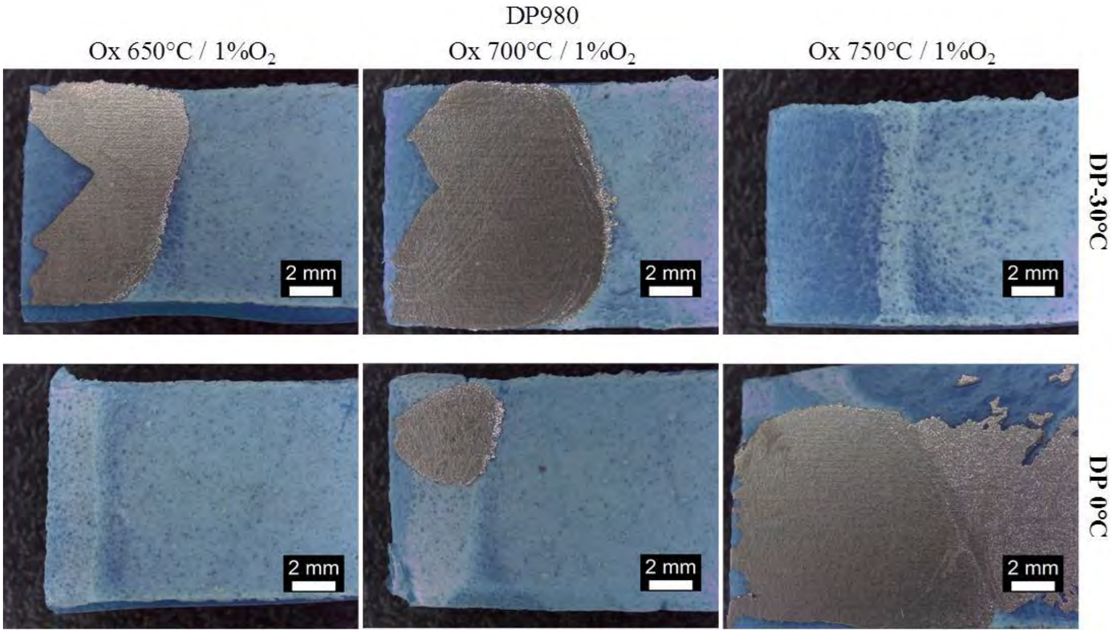

Figure 64: Picture of the glue side after bending.

A better inhibition layer (narrower and higher peaks) is measured by GDOS on the DP980 steel after the oxidation reduction process (Figure 65). No significant difference can however be noticed between the various oxidation conditions, which means that the coating adhesion is not linked with the reactivity during dipping but due to weak interface behind the inhibition layer.

At high dew point, the inhibition layer is quite the same for the DP980 than for the IF-Ti, which should induce only a slight decrease of the wetting behavior during the first second of dipping.

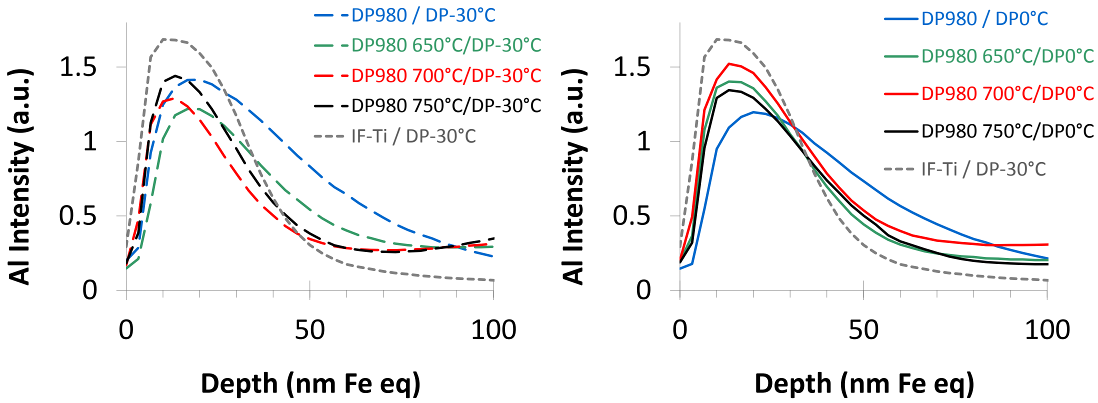

Figure 65: GDOS profile of the Al peak associated with the inhibition layer after hot dipping in the ZM 11/11 bath.

The SEM observation of the inhibition layer (Figure 65) shows a good repartition of fine Fe_2Al_5 crystals for all oxidation conditions, the holes in this layer been probably connected to the ones observed in the reduced iron layer and filled with Mn/Si oxides (Figure 61). Indeed, a clear lack of coverage is observed along grain boundaries were Mn oxides are present before dipping. Unfortunately, the zinc layer removal by electrochemical dissolution also dissolves the selective oxidation. This analysis confirms that the bad adhesion sometime observed (Figure 64) is not related a bad inhibition layer but to a weak steel / coating interface.

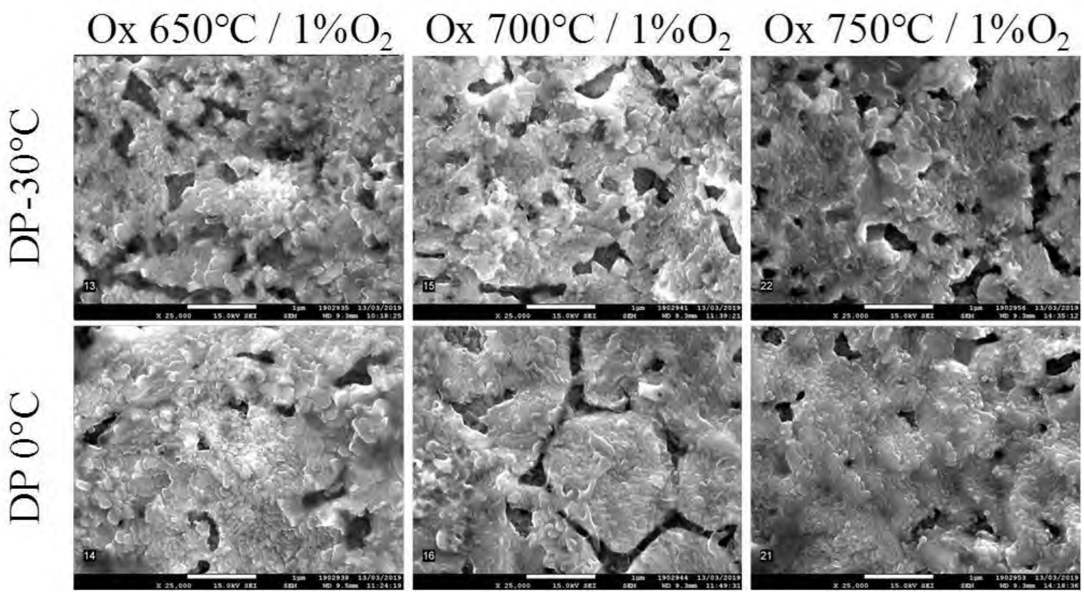

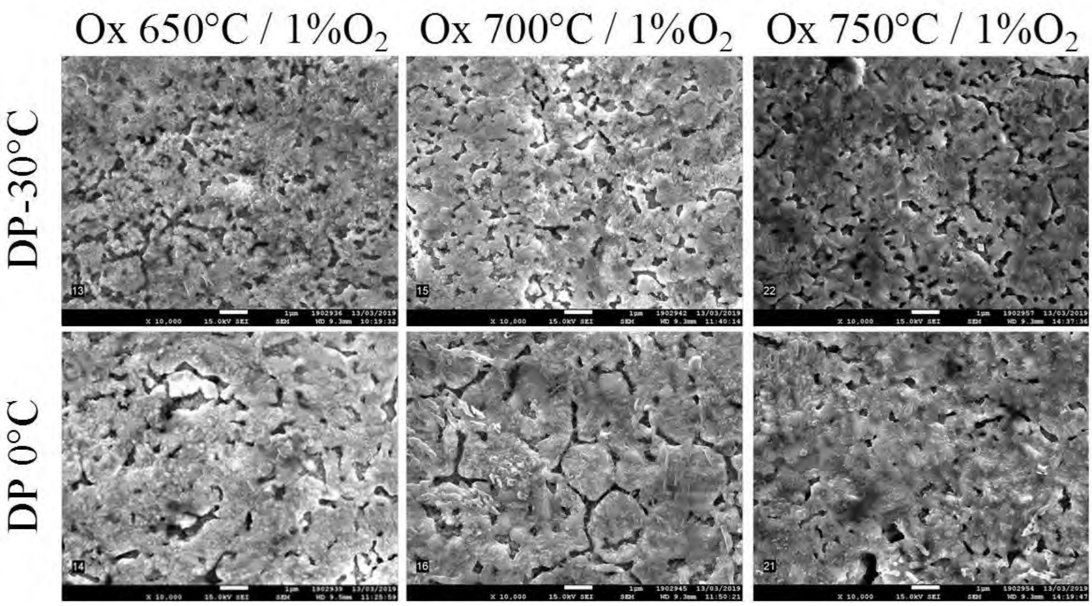

Figure 66: SEM images of the inhibition layer for the DP980 after electrochemical dissolution of the zinc layer

The wetting experiments, reported for the DP980 grade (Figure 67) confirm the strong wetting improvement, the final wetting angle being in this case even better than for the IF Ti steel, especially if the oxidation step is follow by a soaking at high dew point. The wetting, measured during the first 3 seconds are very close to the one obtained for the IF-Ti steel, which is consistent with the previous results reported for the inhibition layer.
This result is in good agreement with the visual observations of the MultiDip panels.

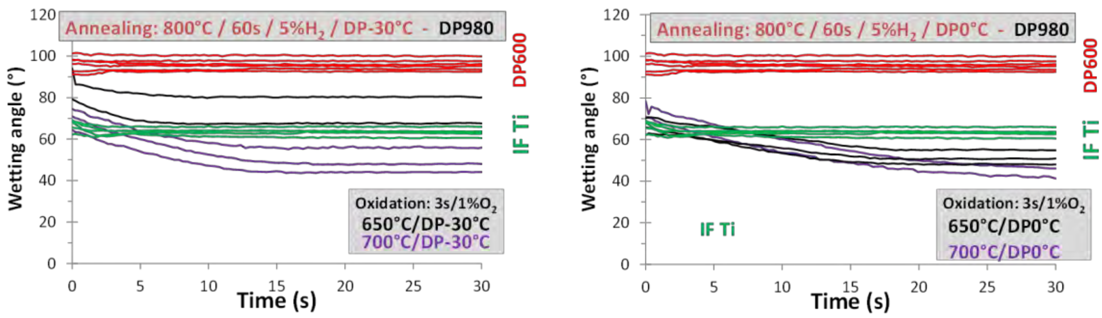

Figure 67: An oxidation step strongly improves the wetting behaviour of the DP980 steel grade. The annealing at high dew point gives an additional effect.

GDOS analyses have been made after a full annealing to better characterize the weak steel / coating interface (Figure 68 to Figure 70). It can be observed that the reduced iron layer is thicker after an oxidation at high temperature (750°C). If this layer is not completely consumed for the formation of the inhibition layer, it can be imagine that this residual reduced iron could form a weak interface. This explanation is however no more valid for the low oxidation temperature (650°C). At this temperature, more Si and Cr oxides are observed at the steel / coating interface, which could also be a weak interface. The same observation can be made after an oxidation at 700°C, but at 750°C, such segregation is associated with a good adhesion.

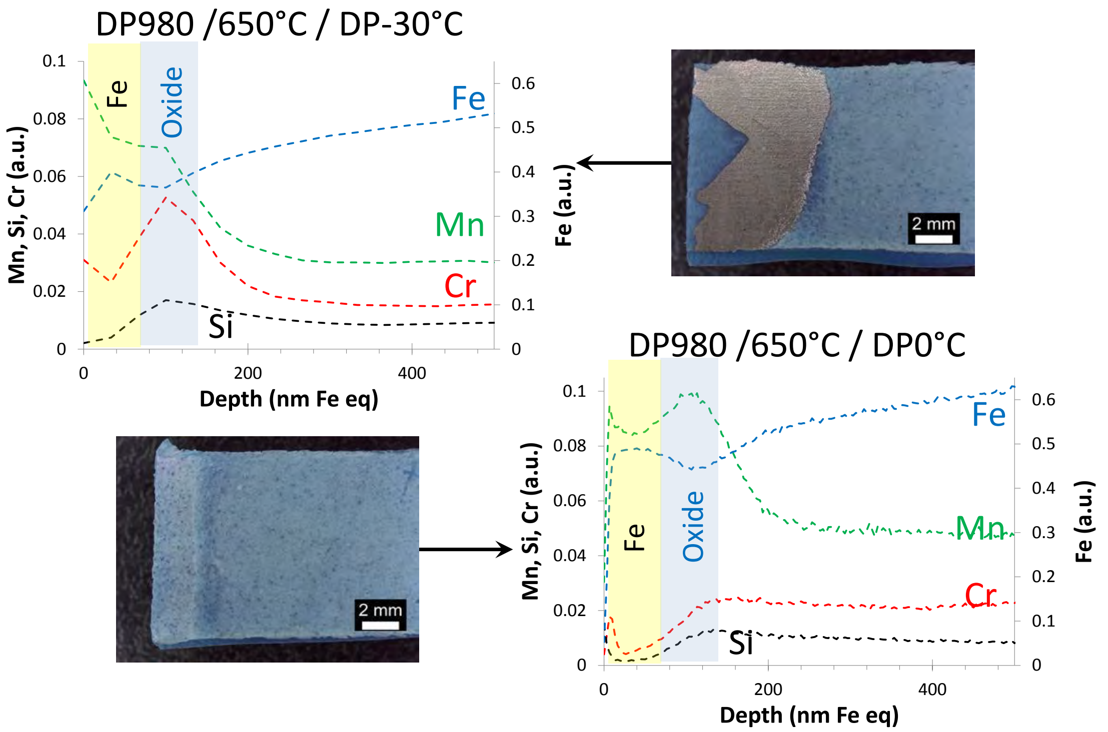

Figure 68: GDOS analyses after an oxidation at 650°C followed by a complete annealing.

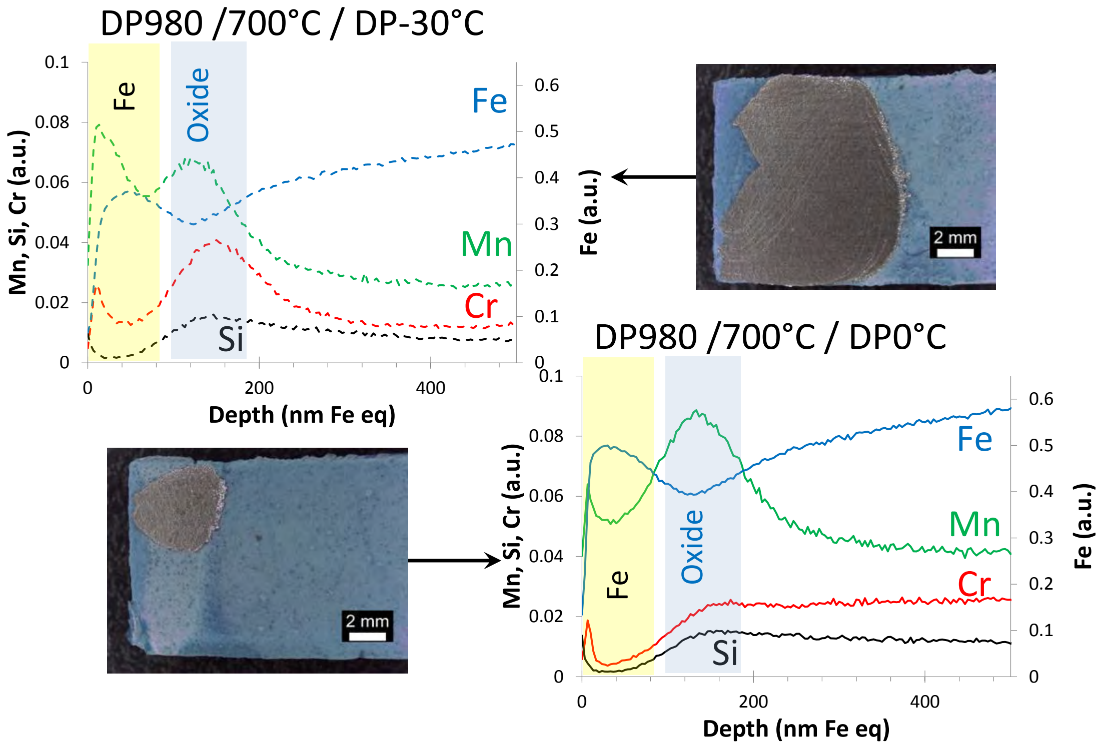

Figure 69: GDOS analyses after an oxidation at 700°C followed by a complete annealing.

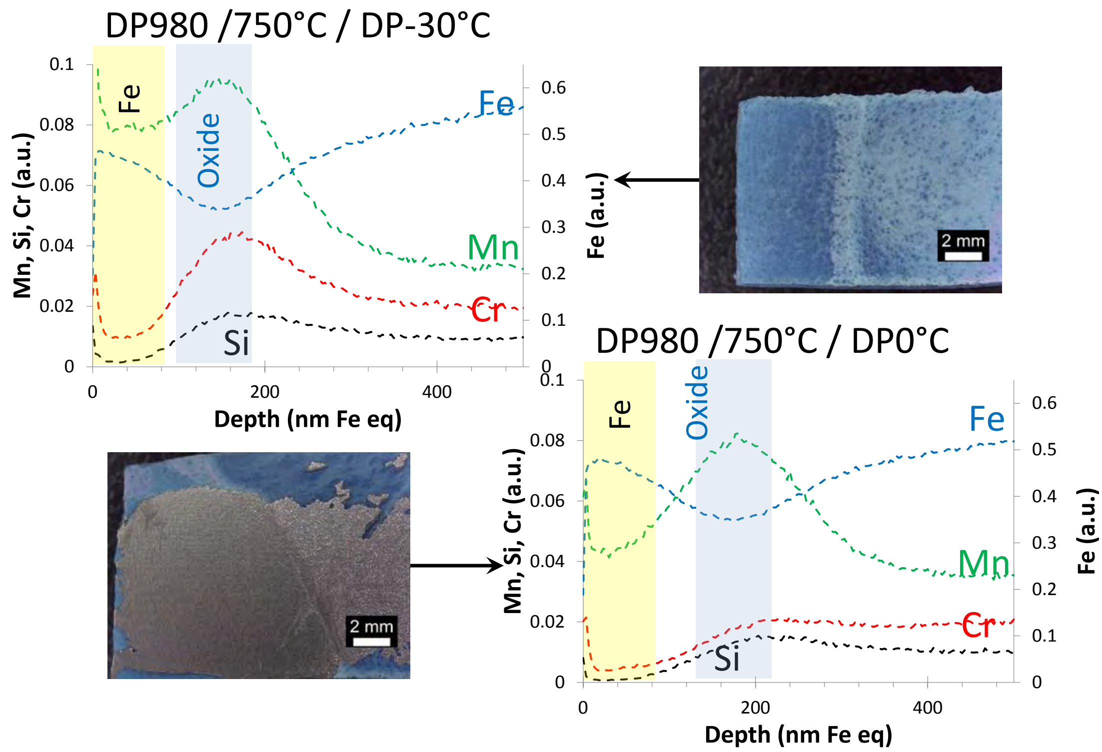

Figure 70: GDOS analyses after an oxidation at 750°C followed by a complete annealing.

SEM analyses have been made on the glue side and on the corresponding steel side in case of bad coating adhesion.

The EDX analyses on the glue side indicate that the Fe_2Al_5 layer has been detached from the steel substrate, but no significant alloying element enrichment can be noticed on the sample side. This however confirms that the interface is the weak area. Some Fe_2Al_5 however remains on the steel surface and some Si oxide is detected on the glue side, which could be linked to the Mn/Si nodules observed after the complete annealing cycle (Figure 61)

In the case of the GI bath, a good coating adhesion was always measured after an oxidation / reduction process. The main difference with the ZM 11/11 bath is the Mg/Al content in the bath, but if a correct inhibition layer is built, the presence Mg and Al oxides over the bath before dipping cannot be an explanation because the failure occurs at the steel / coating interface.

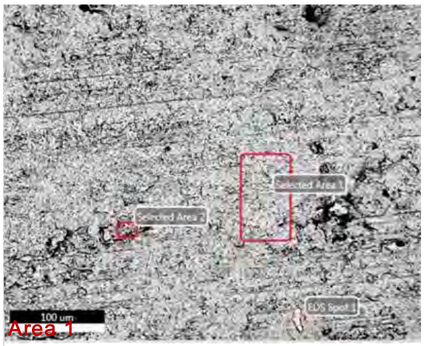

%at	Area 1
Al	1.4
Si	0.8
Cr	0.5
Mn	2.5
Fe	93.1
Zn	1.7

Sample side

%at	DP980
Al	0.10
Si	0.97
Cr	0.36
Mn	2.28

DP980: 800°C/60s/5%H_2/DP-30°C
Oxidation 650°C/1%O_2

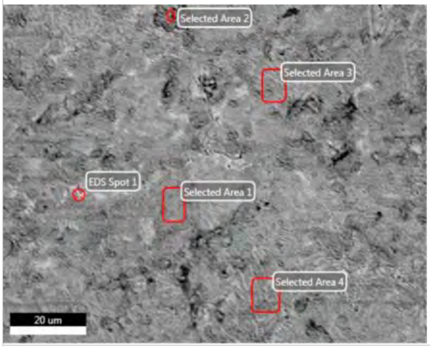

%at	Area 1	Area 2	Area 3	Area 4
O	10.1	7.3	8	8.9
Mg	5.1	5.4	13.1	8.3
Al	16.0	18	10	14.1
Si	0.4	0.5		
Mn	2.7	2.4	1.7	2.1
Fe	17.9	32.5	17.2	22.5
Zn	47.8	33.9	50	44.1

Glue side

Figure 71: SEM – EDX analyses on the steel and the glue side in case of the coating failure for the DP980 at 650°C.

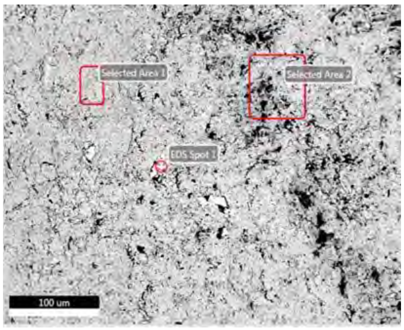

%at	Area 1	Area 2	Spot1
O		7.6	
Al	0.5	1.4	
Si	0.4	1	
Cr	0.5	0.5	
Mn	2.4	2.2	
Fe	94.5	85.9	6.9
Zn	1.7	1.4	93.1

Sample side

DP980: 800°C/60s/5%H_2/DP-30°C
Oxidation 700°C/1%O_2

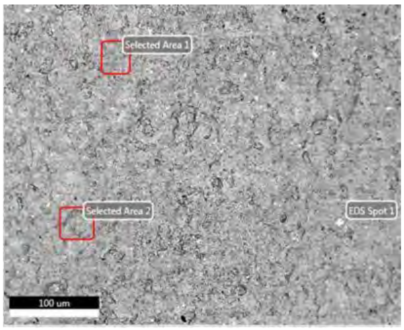

%at	Area 1	Area 2	Spot1
Mg	7.3	7.2	22.7
Al	14.6	13.2	2.5
Si	0.4	0.5	
Mn	2.8	2.7	
Fe	27.2	32.3	
Zn	47.7	44.1	74.8

Glue side

Figure 72: SEM – EDX analyses on the steel and the glue side in case of the coating failure for the DP980 at 700°C.

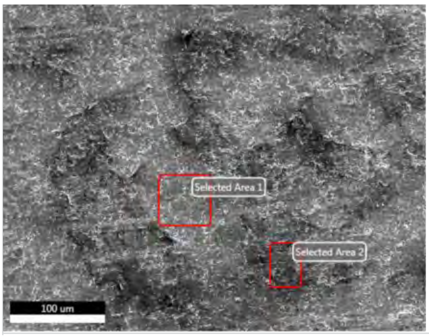

%at	Area 1	Area 2
O	9.8	10
Al	2.0	1.1
Si	0.6	0.7
Mn	2.3	2.3
Fe	83.6	85.1
Zn	1.7	0.8

Sample side

DP980: 800ºC/60s/5%H_2/DP0ºC
Oxidation 750ºC/1%O_2

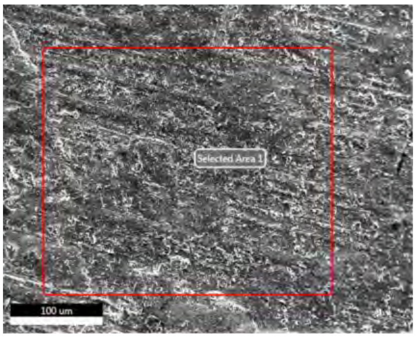

%at	Area 1
Mg	4.1
Al	15.0
Si	0.5
Mn	3.2
Fe	43.0
Zn	34.2

Glue side

Figure 73: SEM – EDX analyses on the steel and the glue side in case of the coating failure for the DP980 at 750°C.

Finally, Auger analyses have also been made to characterise this steel / coating interface. The Auger mapping confirms the presence of MnO along the steel grain boundaries. Some selective oxides are detected inside the inhibition layer but they don't make a continuous film, which cannot explain the bad coating adhesion.

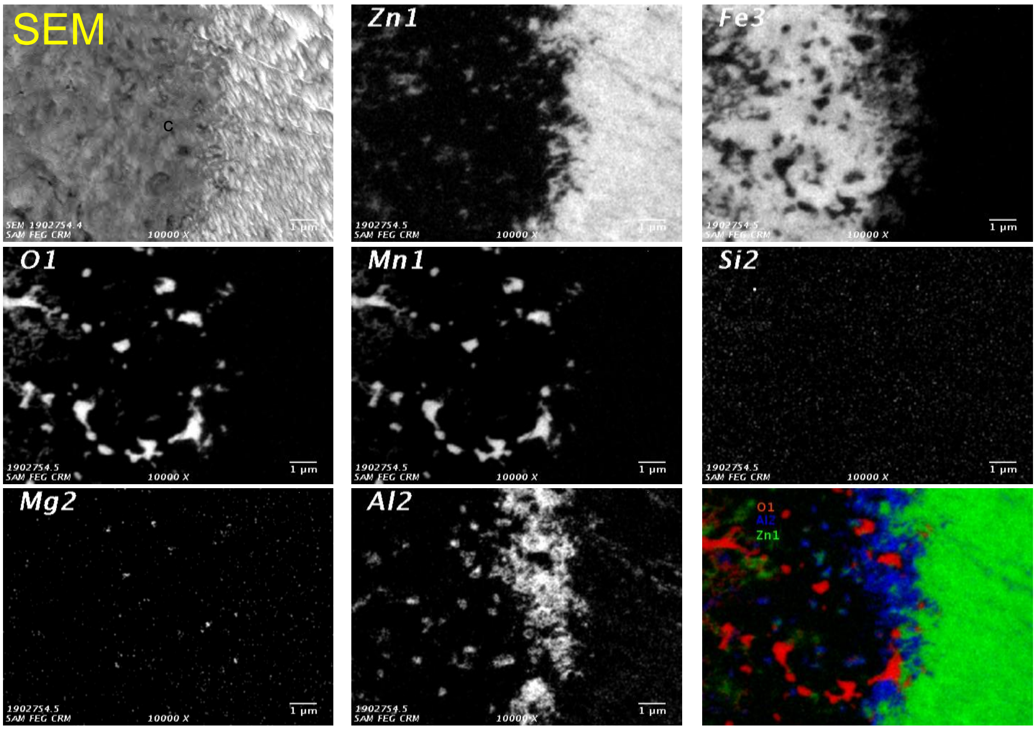

Figure 74: DP980: Auger mapping at the zinc / steel interface: No oxidized Mg observed under the Fe_2Al_5 layer, but some Mn/Si oxides

5.4 Conclusion for the ZM 11/11 bath.

- For the IF Ti: a good coating is obtained after reference annealing conditions ($5\%H_2$/DP-30ºC), the same wettability than GI baths is measured during the first 3 seconds.
- For the DP600:
  - An acceptable coating is achieved after standard annealing ($5\%H_2$/DP-30°C)
  - After annealing at high dew point, the coating quality is significantly improved.
- For the DP980:
  - After standard annealing some bare spots are noticed as well as significant dross flows, which indicates a deterioration of the coatability in comparison with the DP600.
  - After annealing at high dew point, the coating quality is not improved. This is due to the presence of a Mn oxide layer after annealing.
  - Very good coating appearance is noticed after an oxidation / reduction process, but the coating adhesion is only acceptable for some oxidation conditions. No clear explanation can be drawn from the analyses except that this bad adhesion is related to a weak steel/coating interface.
- For the TRIP-Si:
  - Large bath dewetting is observed under reference conditions
  - Acceptable wetting and coating adhesion are measured after annealing at high dew point due to the homogeneous but not continuous Fe_2Al_5 repartition
  - Very good coating appearance is noticed after an oxidation / reduction process, but the coating adhesion is very poor if the oxidation is made above 600°C. The presence of a Si/Mn oxide layer at the steel / coating interface explains this bad adhesion.

6. Conclusions and future work

This work has confirmed that a better coating is generally obtained after annealing at high dew point, but is associated with a significant decarburizing.
The introduction of an oxidation during heating strongly improves zinc wetting but often deteriorates the coating adhesion. Therefore, this oxidation has to made at low temperature (600°C) to limit the Mn/Si segregation along the steel/reduce interface.